Plant Cell Advance Publication. Published on May 30, 2017, doi:10.1105/tpc.17.00136

RESEARCH ARTICLE

Interplay of Plasma Membrane and Vacuolar Ion Channels, Together with BAK1, Elicits Rapid Cytosolic Calcium Elevations in Arabidopsis during Aphid Feeding

Thomas R. Vincent[1], Marieta Avramova[1], James Canham[1], Peter Higgins[2], Natasha Bilkey[2,3], Sam T. Mugford[2], Marco Pitino[2], Masatsugu Toyota[3,4,5], Simon Gilroy[3], Anthony J. Miller[1], Saskia Hogenhout[2*] and Dale Sanders[1*]

[1] Department of Metabolic Biology, John Innes Centre, Norwich Research Park, Norwich, UK.
[2] Department of Cell and Developmental Biology, John Innes Centre, Norwich Research Park, Norwich, UK.
[3] Department of Botany, University of Wisconsin, Madison, WI, USA.
[4] Department of Biochemistry and Molecular Biology, Saitama University, 255 Shimo-Okubo, Sakura-ku, Saitama, 338-8570, Japan.
[5] Japan Science and Technology Agency (JST), Precursory Research for Embryonic Science and Technology (PRESTO), 4-1-8 Honcho, Kawaguchi, Saitama, 332-0012, Japan.
*Corresponding authors: Saskia.Hogenhout@jic.ac.uk, Dale.Sanders@jic.ac.uk

Short title: Aphids elicit rapid plant calcium elevations

One-sentence summary: During feeding by aphids in vivo, a fluorescent calcium sensor reveals a mesophyll calcium signal that is dependent on BAK1, GLR3.3/GLR3.6 and TPC1.

The author responsible for distribution of materials integral to the findings presented in this article in accordance with the policy described in the Instructions for Authors (www.plantcell.org) is: Dale Sanders (Dale.Sanders@jic.ac.uk).

ABSTRACT

A transient rise in cytosolic calcium ion concentration is one of the main signals used by plants in perception of their environment. The role of calcium in the detection of abiotic stress is well documented; however, its role during biotic interactions remains unclear. Here, we use a fluorescent calcium biosensor (GCaMP3) in combination with the green peach aphid (*Myzus persicae*) as a tool to study *Arabidopsis thaliana* calcium dynamics *in vivo* and in real time during a live biotic interaction. We demonstrate rapid and highly-localised plant calcium elevations around the feeding sites of *M. persicae*, and by monitoring aphid feeding behaviour electrophysiologically we demonstrate that these elevations correlate with aphid probing of epidermal and mesophyll cells. Furthermore, we dissect the molecular mechanisms involved, showing that interplay between the plant defence co-receptor BRASSINOSTEROID INSENSITIVE-ASSOCIATED KINASE 1 (BAK1), the plasma membrane ion channels GLUTAMATE RECEPTOR-LIKE 3.3 and 3.6 (GLR3.3 and GLR3.6) and the vacuolar ion channel TWO-PORE CHANNEL 1 (TPC1) mediate these calcium elevations. Consequently, we identify a link between plant perception of biotic threats by BAK1, cellular calcium entry mediated by GLRs, and intracellular calcium release by TPC1 during a biologically relevant interaction.

INTRODUCTION

Transient rises in cytosolic calcium ion concentration ($[Ca^{2+}]_{cyt}$) act as ubiquitous signals that coordinate a range of physiological processes in plants. The capacity for abiotic stresses such as cold, salt and drought to elicit $[Ca^{2+}]_{cyt}$ elevations in plants has been known for some time (Knight et al., 1991; McAinsh et al., 1995; Allen et al., 2000; Kiegle et al., 2000). Biotic stresses such as plant pathogens can also elicit $[Ca^{2+}]_{cyt}$ elevations; however, the study of these elevations has been largely restricted to the use of elicitors as opposed to live organisms (Blume et al., 2000; Lecourieux et al., 2005; Thor and Peiter, 2014; Keinath et al., 2015; Charpentier et al., 2016). Conversely, although application of live chewing insects elicits large $[Ca^{2+}]_{cyt}$ elevations, these are hard to differentiate from those caused by wounding alone (Verrillo et al., 2014; Kiep et al., 2015). The green peach aphid (*Myzus persicae*), which pierces a small number of plant cells (Will and van Bel, 2006), offers a unique opportunity to study plant Ca^{2+} dynamics *in vivo* during a biotic stress more akin to plant-microbe interactions.

Plant perceive detrimental biotic events through the detection of conserved pathogen/herbivore-associated molecular patterns (PAMPs/HAMPs), by pathogen recognition receptors (PRRs) in the plant (Chinchilla et al., 2006; Zipfel et al., 2006; Yamaguchi et al., 2006; Miya et al., 2007), many of which interact with the defence co-receptor BRASSINOSTEROID INSENSITIVE1-ASSOCIATED KINASE1 (BAK1) (Chinchilla et al., 2007; Heese et al., 2007) during response known as PAMP-triggered immunity (PTI) (Jones and Dangl, 2006; Zipfel, 2009; Mithofer and Boland, 2008). One of the earliest events upon pathogen recognition is a transient elevation in $[Ca^{2+}]_{cyt}$ (Blume et al., 2000; Lecourieux et al., 2005; Keinath et al., 2015), whilst a

hallmark of symbiotic biotic interactions is [Ca^{2+}] oscillations in the nucleus (Ehrhardt et al., 1996; Kosuta et al., 2008). Despite this, the mechanisms underlying $[Ca^{2+}]_{cyt}$ elevations during biotic interactions have remained unclear, although several Ca^{2+}-permeable channels have been suggested to play a role. The CYCLIC NUCLEOTIDE GATED CHANNEL (CNGC) and GLUTAMATE RECEPTOR-LIKE CHANNEL (GLR) families include some of the best-characterised plasma membrane Ca^{2+}-permeable channel families in plants (Dodd et al., 2010). CNGC15 facilitates nuclear [Ca^{2+}] oscillations in response to symbiotic elicitors (Charpentier et al., 2016), whilst CNCG2 mediates entry of Ca^{2+} from the apoplast (Wang et al., 2017) and the *CNGC2*-null mutant *defence no death 1* (*dnd1*) exhibits a constitutive defence phenotype (Yu et al., 1998; Clough et al., 2000). Furthermore, *GLR3.3* and *GLR3.6* have been implicated in systemic signalling during wounding (Mousavi et al., 2013; Salvador-Recatala, 2016). In addition, herbivory-elicited Ca^{2+} signals are attenuated in null mutants of the vacuolar channel *TWO-PORE CHANNEL 1* (*TPC1*) (Kiep et al., 2015). TPC1 is a tonoplast-localised Ca^{2+}-permeable channel whose activity is regulated by voltage and Ca^{2+} (Hedrich and Neher, 1987; Ward and Schroeder, 1994; Peiter et al., 2005; Gradogna et al., 2009; Guo et al., 2016; Kintzer and Stroud, 2016; Guo et al., 2017). TPC1 also has an established role in systemic Ca^{2+} signalling in response to salt stress (Choi et al., 2014; Evans et al., 2016) and wounding (Kiep et al., 2015) via its positive regulation by Ca^{2+} in a process termed Ca^{2+}-induced Ca^{2+} release. However, the mechanism by which Ca^{2+}-induced Ca^{2+} release is triggered in plants remains unknown.

M. persicae is a significant agricultural pest due to its highly polyphagous nature (Blackman and Eastop, 2000; Schoonhoven et al., 2005; Blackman and

Eastop, 2007; Mathers et al., 2017). Aphids pierce plant tissue using specialised mouthparts, called stylets, to establish long-term feeding from the phloem (Dixon, 1998). On the route to the phloem, the stylets navigate between epidermal and mesophyll cells, occasionally penetrating these cells during a process known as the pathway feeding phase (Tjallingii, 1985; Tjallingii and Esch, 1993). The ability of an aphid to feed successfully on a plant appears to be partly determined during these penetrations, as the pathway phase still occurs with aphid species unable to establish long-term feeding (Chen et al., 1997; Sauge et al., 1998; Jaouannet et al., 2015; Nam and Hardie, 2012). Furthermore, as with microbial pathogens, aphids are detected through a BAK1-dependent mechanism, although the PRRs involved have remained elusive, with FLAGELLIN-SENSITIVE 2 (FLS2), EF-TU RECEPTOR (EFR), CHITIN ELICITOR RECEPTOR KINASE 1 (CERK1), PEP1 RECEPTOR 1 (PEPR1) and PEP1 RECEPTOR 2 (PEPR2) not appearing to play a role (Prince et al., 2014; Chaudhary et al., 2014).

There is circumstantial evidence that Ca^{2+} signalling is relevant to plant–aphid interactions. The majority of plant gene expression studies performed after infestation with aphids reveal a significant over-representation of Ca^{2+} signalling-related transcripts, most of which display upregulation (Foyer et al., 2015). In addition, feeding by *M. persicae* elicits plasma membrane depolarisations in Arabidopsis mesophyll cells (Bricchi et al., 2012), and Ca^{2+}-selective microelectrodes detect a significant Ca^{2+} flux out of the extracellular space into tobacco mesophyll cells after infestation with *M. persicae* (Ren et al., 2014). However, the primary role of Ca^{2+} in plant-aphid interactions is believed to be in the phloem, where it is hypothesised to have a function in signalling by promoting occlusion via regulation of

callose production (Kauss et al., 1983; Singh and Paolillo, 1990; Aidemark et al., 2009) and plugging by phloem proteins (Knoblauch et al., 2001; Knoblauch et al., 2003; Furch et al., 2009). Furthermore, it has been suggested that proteins in aphid saliva act to chelate phloem Ca^{2+} to prevent occlusion. Indeed, aphid saliva contains Ca^{2+}-binding proteins (Will et al., 2007; Carolan et al., 2009; Rao et al., 2013) and application of saliva to legume phloem-plugging proteins results in their contraction (Will et al., 2007). Aphid saliva also contains effector molecules that suppress plant defence (Bos et al., 2010; Pitino and Hogenhout, 2013; Atamian et al., 2013; Naessens et al., 2015; Wang et al., 2015; Kettles and Kaloshian, 2016), as observed with microbial pathogens (Jones and Dangl, 2006; Galan et al., 2014) and chewing insects (Musser et al., 2002).

To date, there have been no direct measurements of local $[Ca^{2+}]_{cyt}$ dynamics in a leaf when only a few cells are under biotic attack. Aphids offer an approach by which to study such dynamics, because the stylets of these insects probe individual plant cells, and this behaviour can be monitored electrophysiologically (Tjallingii, 1985; Tjallingii and Esch, 1993). Here, using transgenic Arabidopsis plants expressing the GFP-based Ca^{2+} sensor GCaMP3 (Tian et al., 2009), we were able to show that aphid probing of epidermal and mesophyll cells elicits rapid and highly localised $[Ca^{2+}]_{cyt}$ elevations around aphid feeding sites. We found that these $[Ca^{2+}]_{cyt}$ elevations depend on *BAK1*, *GLR3.3/GLR3.6* and *TPC1*, indicating that $[Ca^{2+}]_{cyt}$ is produced as part of a cellular PTI response and is then propagated via the influx of extracellular and vacuolar Ca^{2+} and interplay between Ca^{2+}-permeable channels.

150

RESULTS

Aphids elicit rapid and highly-localised $[Ca^{2+}]_{cyt}$ elevations in Arabidopsis

Although other single wavelength Ca^{2+} sensors have been used in plants, including Case12 (Zhu et al., 2010) and RGECO (Keniath et al., 2015), we chose to apply GCaMP3, a Ca^{2+}-responsive probe that combines a large dynamic range, photostability, and compatibility with standard GFP-based imaging equipment (Tian et al., 2009). In addition, the assay for imaging calcium dynamics around aphid feeding requires relatively low magnification to capture the final feeding site selected by the insect without disturbing (moving) the sample. We have found the ease of detection and compatibility with the stereo-fluorescence microscopy makes this probe superior for these assays when compared to, e.g., the ratiometric yellow cameleon Ca^{2+} sensors (e.g., Choi et al., 2014) that need more sophisticated ratio imaging equipment such as a confocal microscope for accurate quantification.

To assess whether $[Ca^{2+}]_{cyt}$ elevations are seen in *35S:GCaMP3* Arabidopsis plants during *M. persicae* feeding, a single leaf assay was developed. This assay was set up by detaching leaves from *35S:GCaMP3* plants and floating leaves on water inside single wells of a 96-well plate. Because wounding induces Ca^{2+} signals in leaves (Kiep et al., 2015), the single leaves were detached and placed into plates 24 h prior to the start of microscopy experiments to allow wound-induced Ca^{2+} signals to dissipate. The floating leaf assay prevented aphid escape from the wells and allowed standardization of the assay by restricting aphid feeding to the abaxial surface of leaves of similar developmental stages.

Upon transferring a *M. persicae* individual to a *35S:GCaMP3* leaf, a clear increase in GCaMP3 (GFP) fluorescence was observed around the feeding site (Figure 1A; Supplemental Movie 1), which indicated a rise in $[Ca^{2+}]_{cyt}$ (Tian et al., 2009). This rise was consistent and significantly greater than the fluorescence in equivalent locations on no-aphid control leaves (Figure 1B). Typically, the fluorescence burst was generated within 95 s upon settling of the aphids (Figure 1B, Supplemental Movie 1), with settling defined as an aphid remaining stationary for 5 min. From a total of 33 observations, the average area of the $[Ca^{2+}]_{cyt}$ elevation was 110 ± 18 μm^2 and the leading wave front of this elevation travelled radially at 5.9 ± 0.6 µm/s from its centre. Although variation in the raw GFP fluorescence (F) could be observed between leaves under the microscope (e.g. Supplemental Movie 1, Figure 1A), for quantitative analysis this was accounted for by normalising the GFP fluorescence to the baseline fluorescence before the aphid settled ($\Delta F/F$ – Figure 1B).

The aphid-elicited increase in fluorescence was not detected in regions of the leaf systemic to the feeding site (Figure 2). It has been shown previously that it is possible to detect systemic $[Ca^{2+}]_{cyt}$ elevations in detached leaves in response to salt stress (Xiong et al., 2014), suggesting that detachment of leaves does not prohibit the detection of systemic signals. Furthermore, whole plants exposed to aphids also exhibited $[Ca^{2+}]_{cyt}$ elevations, although a high number of replicates was not possible as it proved to be challenging to track aphid movement on a whole plant (Supplemental Movie 2). By contrast, the detached leaf assay was capable of detecting changes in $[Ca^{2+}]_{cyt}$ around the aphid feeding site in a robust and repeatable manner. Indeed, confocal microscopy confirmed that GCaMP fluorescence was present primarily in the cytosol and not within the vacuole,

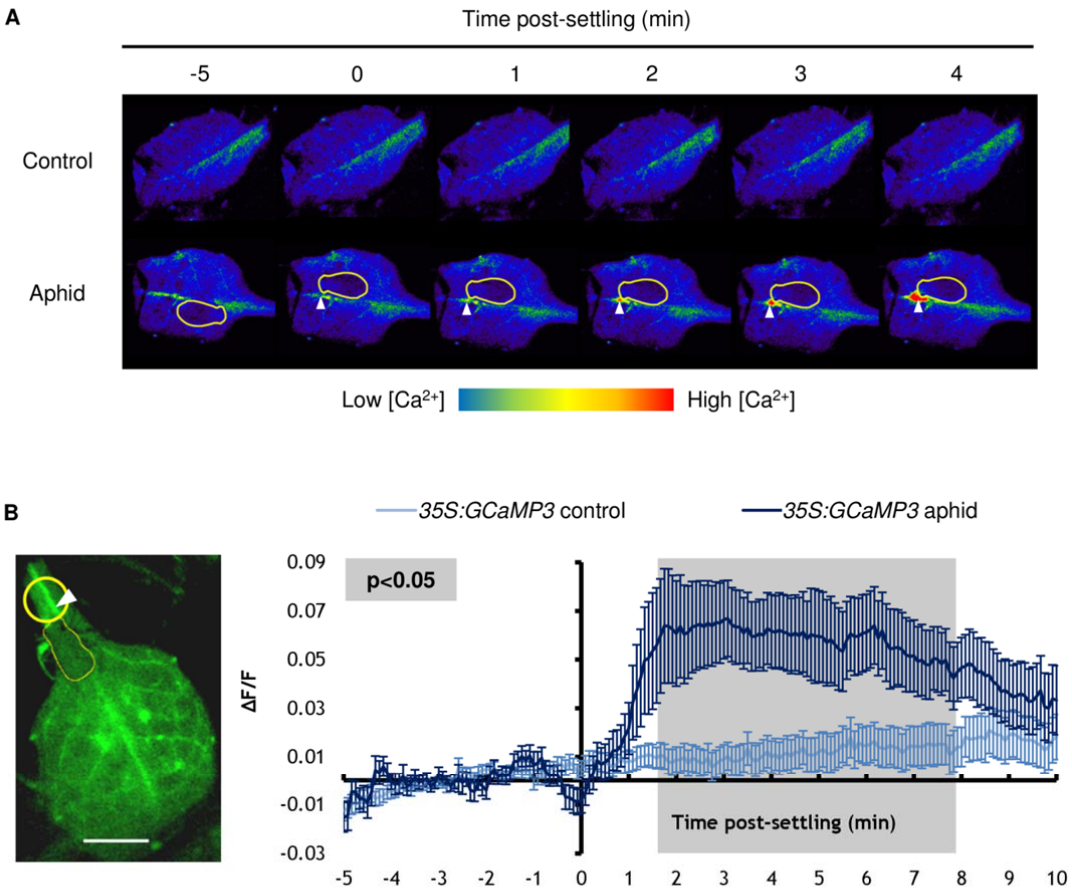

Figure 1. The GCaMP3 sensor detects $[Ca^{2+}]_{cyt}$ elevations around the aphid feeding site on detached leaves.

A) Representative stereo-microscope images showing GFP fluorescence (colour coded according to the inset scale) around feeding sites of leaves exposed to a *M. persicae* adult at several time points after aphid settling. Aphid outlined in yellow. Location of feeding site indicated with an arrowhead.

B) Left: stereo-microscope image of a feeding site region (yellow circle) used for the analyses shown on the right (scale bar = 1 mm). Aphid outlined in yellow and location of feeding site indicated with an arrowhead. Right: normalised GFP fluorescence (ΔF/F) measurements every 5 s around the feeding site from 5 min before until 10 min after settling of an adult aphid. F, average fluorescence intensity prior to aphid settling (baseline); ΔF, difference between measured fluorescence and baseline fluorescence. Error bars represent the standard error of the mean (SEM, n=34). The average area of the $[Ca^{2+}]_{cyt}$ elevation was 110±18 μm² and the leading wave front of this elevation travelled radially at 5.9 ±0.6 μm/s from its centre. Grey shading indicates a significant difference between treatments using a Student's t-test within a general linear model (GLM) at $p<0.05$.

200 although the presence of the GCAMP3 sensor within the nucleus could not be

201 excluded (Supplemental Figure 1).

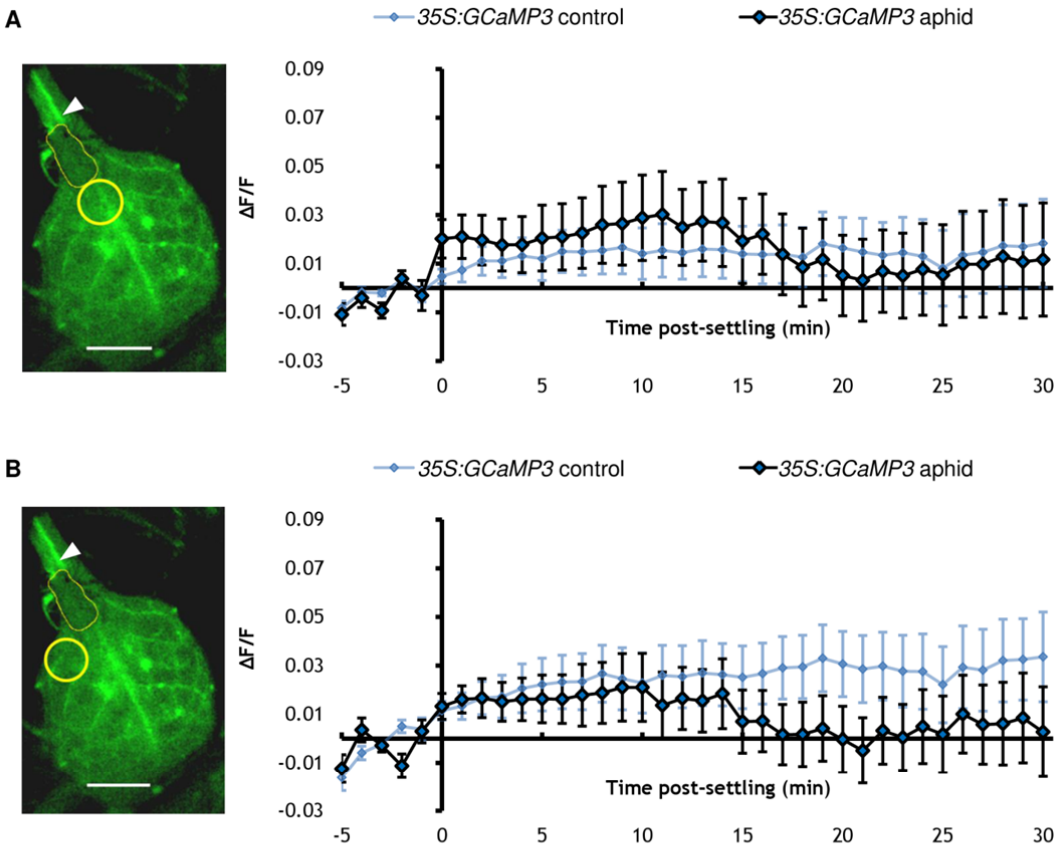

Figure 2. The GCaMP3 sensor does not detect $[Ca^{2+}]_{cyt}$ elevations systemic to the aphid-feeding site.

A) Left: stereo-microscope image of a leaf exposed to an aphid with the yellow circle indicating the midrib region systemic to the feeding site (arrowhead) of an aphid (outlined in yellow). Scale bar = 1 mm. Right: normalized fluorescence (ΔF/F) at midrib regions systemic to the aphid feeding sites (as exemplified with the yellow circle in the image on the left) of *35S:GCaMP3* leaves exposed to *M. persicae* adults and no-aphid controls. Error bars represent SEM (n=34). Data from aphid responding leaves are not significantly different from controls (Student's t-test within a GLM, $p>0.05$).

B) Left: stereo-microscope image of a leaf exposed to an aphid with the yellow circle indicating the lateral tissue regions (next to the midrib) systemic to the feeding site (arrowhead) of an aphid (outlined in yellow). Right: ΔF/F at lateral tissue regions systemic to the aphid-feeding sites (as exemplified with the yellow circle in the image on the left) of *35S:GCaMP3* leaves exposed to *M. persicae* adults and no-aphid controls. Error bars represent SEM (n=34). Data from aphid responding leaves are not significantly different from controls (Student's t-test within a GLM, $p>0.05$).

Aphid-induced $[Ca^{2+}]_{cyt}$ elevations occur during probing of the epidermal and mesophyll cells

To investigate where the aphid stylets induce plant $[Ca^{2+}]_{cyt}$ elevations, the aphid stylet behaviour was monitored using the Electrical Penetration Graph (EPG) technique (Tjallingii, 1978; Salvador-Recatala and Tjallingii, 2015). In this technique, the stylet penetrations of epidermal and mesophyll cells during the pathway phase versus the phloem feeding phase can be monitored as distinct changes in voltage output (Figure 3). From 22 observations on soil-grown plants, the first cell punctures occurred at 31 ± 11 s after the beginning of the pathway phase, with the phloem being accessed after 24 ± 3 min (Figure 3A). An adapted version of the EPG technique to assess feeding behaviour on detached *35S:GCaMP3* leaves floating in water showed that the timing of the pathway and phloem feeding phases of aphids on detached *35S:GCaMP3* leaves were comparable to those of soil-grown Col-0 plants, with the pathway phase lasting for 15-25 min (Figure 3B). In both EPG assays, the pathway phases began very rapidly upon aphid settling (Figure 3) and within the timeframe of the aphid-induced $[Ca^{2+}]_{cyt}$ elevation (Figure 1B). Thus, the aphid-induced $[Ca^{2+}]_{cyt}$ elevations mostly likely occur during the pathway phase when the aphid stylets probe epidermal and mesophyll cells.

Ca^{2+} is hypothesised to play a role in the phloem during plant-aphid interactions (Will et al., 2007). To investigate whether an aphid-elicited $[Ca^{2+}]_{cyt}$ elevation occurs in the phloem, the GCaMP3 sensor was expressed under control of the *SUCROSE-PROTON SYMPORTER 2* (*SUC2pro*) promoter (Stadler and Sauer, 1996). In contrast to the *35S:GCaMP3* leaves, *SUC2pro:GCaMP3* leaves did not show aphid-elicited $[Ca^{2+}]_{cyt}$ elevations, though there was a gradual increase in

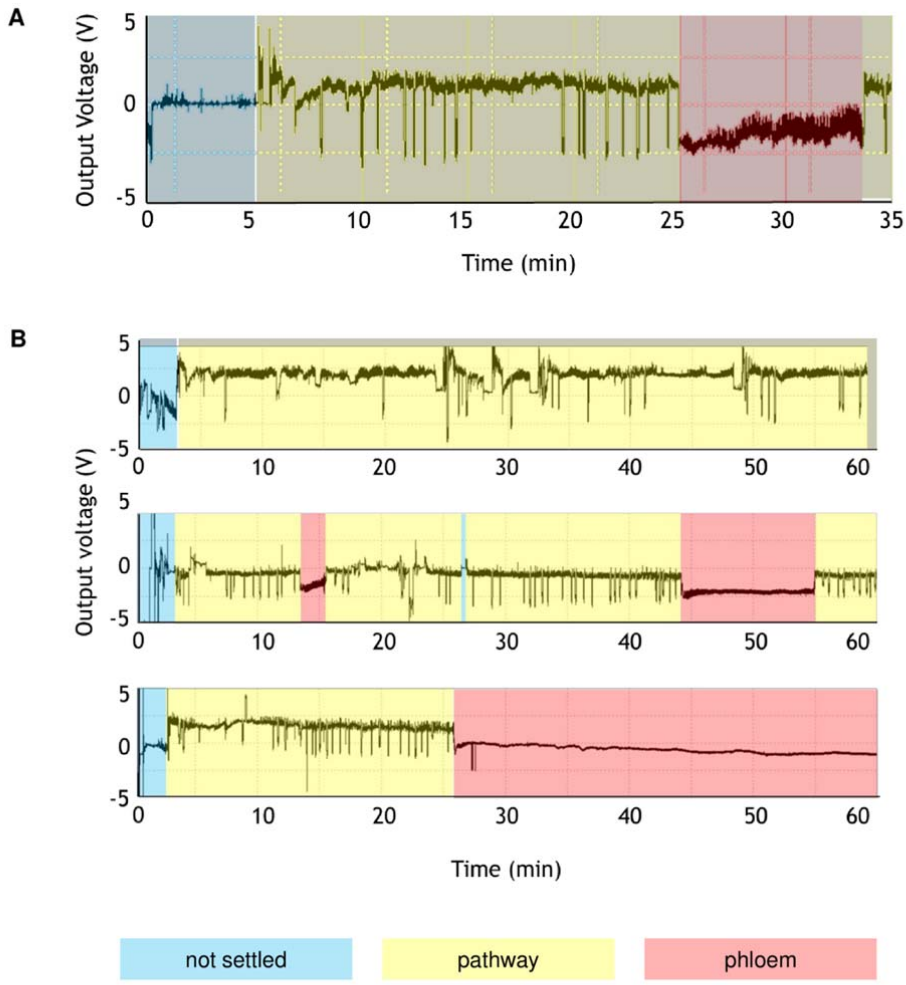

Figure 3. The pathway phase that includes aphid probing of epidermal and mesophyll cells starts immediately upon aphid settling.
Feeding phases represented by coloured shading.

A) Representative EPG trace from an aphid feeding on a whole Col-0 Arabidopsis plant. The first cell puncture occurred at 31 ± 11 s after the beginning of pathway phase, with the phloem accessed after 24 ± 3 min (n=22).

B) Representative EPG traces from aphids feeding on detached *35S:GCaMP3* leaves (n=6).

228 fluorescence over time that occurred independently of the presence of aphids
229 (Figure 4, Supplemental Movie 3). In addition, cold shock is a well-characterised

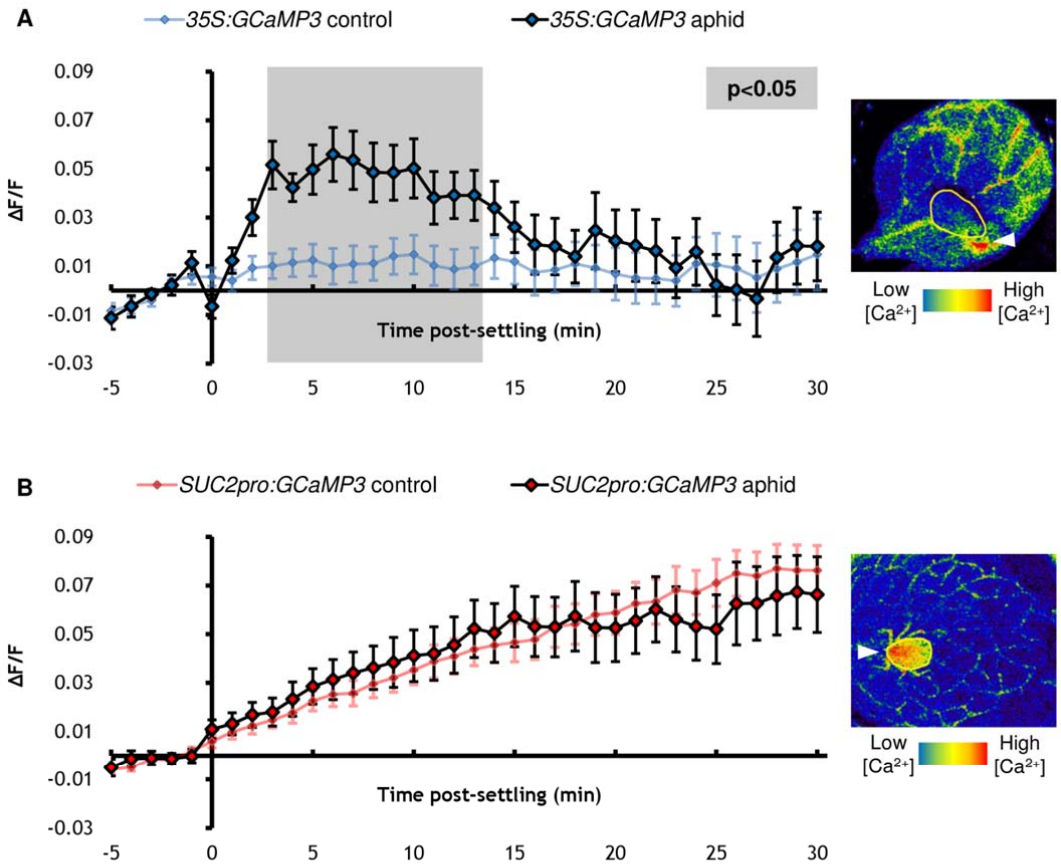

Figure 4. $[Ca^{2+}]_{cyt}$ elevations are not detected in the phloem around aphid feeding sites.

A) Left: normalized fluorescence (ΔF/F) around aphid-feeding sites of *35S:GCaMP3* aphid-exposed leaves and no-aphid controls. Error bars represent SEM (n=31). Grey shading indicates significant difference between treatments (Student's t-test within GLM at $p<0.05$). Right: representative stereo microscope image of a $[Ca^{2+}]_{cyt}$ elevation seen around an aphid-feeding site on a *35S:GCaMP3* leaf. GFP fluorescence is colour-coded according to the inset scale. Aphid outlined in yellow and feeding site indicated with an arrowhead. Image taken at 3 min post-settling.

B) Left: ΔF/F around the aphid-feeding sites of *SUC2pro:GCaMP3* aphid-exposed leaves and no-aphid controls. Error bars represent SEM (n=34). Right: representative stereo microscope image of the absence of $[Ca^{2+}]_{cyt}$ elevation around an aphid-feeding site on a *SUC2pro:GCaMP3* leaf. GFP fluorescence is colour-coded according to the inset scale. Aphid outlined in yellow and feeding site indicated with an arrowhead. Image taken at 3 min post-settling.

230 elicitor of Ca^{2+} signals in plants (Knight et al., 1996; Knight and Knight, 2000; Kiegle
231 et al., 2000). Therefore, to confirm that the *SUC2pro:GCaMP3* construct was

capable of reporting changes in phloem Ca^{2+} dynamics, *SUC2pro:GCaMP3* leaves were treated with cold water (Knight et al., 1996; Knight and Knight, 2000; Kiegle et al., 2000) and showed a clear increase in GFP fluorescence (Supplemental Movie 4). Thus, it does not appear that *M. persicae* elicits $[Ca^{2+}]_{cyt}$ elevations in the Arabidopsis phloem.

Aphid elicitation of $[Ca^{2+}]_{cyt}$ is dependent on BAK1 and GLR3.3/GLR3.6

BAK1 is a defence co-receptor required for PTI against microbes (Chinchilla et al., 2007; Heese et al., 2007) and aphids (Prince et al., 2014; Chaudhary et al., 2014). Thus, to establish whether the aphid-elicited $[Ca^{2+}]_{cyt}$ elevation is a component of PTI, *35S:GCaMP3*-expressing plants were crossed with the *BAK1* null mutant *bak1-5*. The *bak1-5* mutant was selected as it displays defects in immune signalling, but not in brassinosteroid signalling as seen with other *BAK1* mutants (Schwessinger et al., 2011). Whereas *35S:GCaMP3* leaves exhibited the characteristic $[Ca^{2+}]_{cyt}$ elevations around aphid feeding site (Figure 5A), these $[Ca^{2+}]_{cyt}$ elevations were abolished in leaves of *35S:GCaMP3* x *bak1-5* line (Figure 5B, Figure 5C, Supplemental Movie 5). Thus, BAK1 is required for inducing $[Ca^{2+}]_{cyt}$ elevations around aphid feeding sites.

The plasma membrane cation-permeable channels *GLR3.3* and *GLR3.6* have recently been implicated in the Arabidopsis wound response, with systemic electrical signals migrating via the phloem being attenuated in the *GLR* double mutant *glr3.3 glr3.6* (Mousavi et al., 2013). To investigate if these channels also have a role in the more local systemic spread around the aphid feeding sites, we generated a *35S:GCaMP3* x *glr3.3 glr3.6* line. The aphid-induced $[Ca^{2+}]_{cyt}$ elevation was also

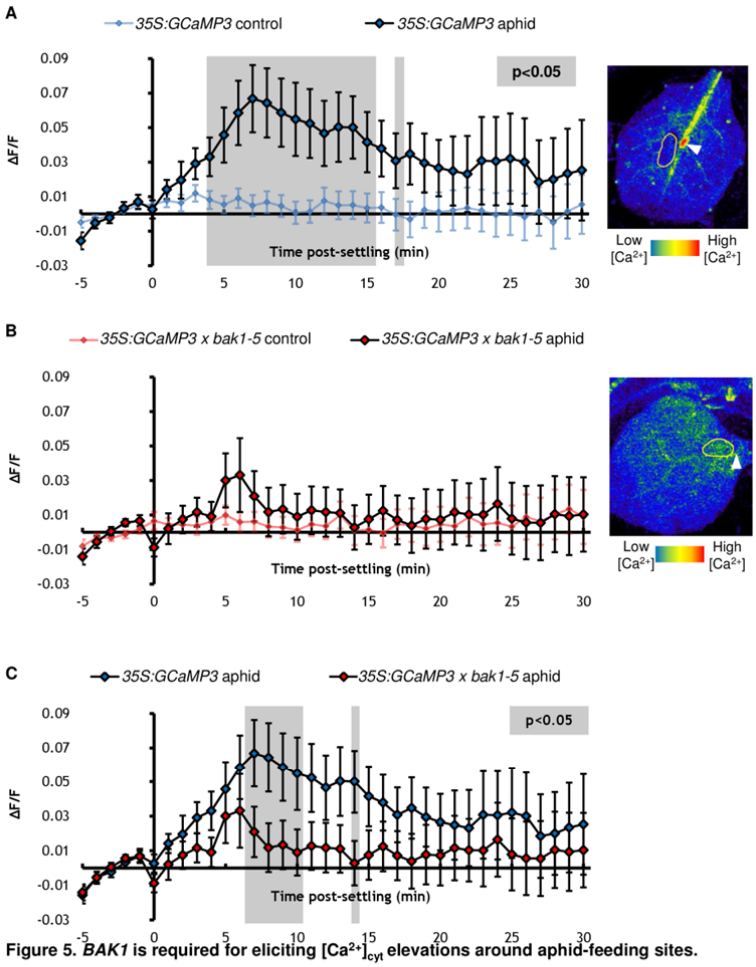

Figure 5. *BAK1* is required for eliciting $[Ca^{2+}]_{cyt}$ elevations around aphid-feeding sites.

A) Left: normalized fluorescence (ΔF/F) around feeding sites of *35S:GCaMP3* aphid-exposed leaves and no-aphid controls. Error bars represent SEM (n=30). Grey shading indicates significant difference between treatments (Student's t-test within GLM at p<0.05). Right: representative stereo-microscope image of the $[Ca^{2+}]_{cyt}$ elevation seen around an aphid-feeding site of a *35S:GCaMP3* leaf. GFP fluorescence colour-coded according to the inset scale. Aphid outlined in yellow and feeding site indicated with an arrowhead. Image taken at 2 min post-settling

B) Left: ΔF/F around feeding sites of *35S:GCaMP3 x bak1-5* aphid-exposed leaves and no-aphid controls. Error bars represent SEM (n=34). Right: representative stereo-microscope image of the absence of $[Ca^{2+}]_{cyt}$ elevation around an aphid-feeding site of a *35S:GCaMP3 x bak1-5* leaf. GFP fluorescence colour-coded according to the inset scale. Aphid outlined in yellow and feeding site indicated with an arrowhead. Image taken at 2 min post-settling.

C) Comparison of ΔF/F around feeding sites of aphid-exposed *35S:GCaMP3* and *35S:GCaMP3 x bak1-5* leaves. Data of aphid exposures shown in panels A and B were replotted together. Areas shaded in grey indicate significant differences between the two treatments (Student's t-test within GLM at p<0.05).

257 abolished in this line (Figure 6, Supplemental Movie 6). These data indicate that
258 *GLR3.3* and *GLR3.6* are required for inducing $[Ca^{2+}]_{cyt}$ elevations around aphid

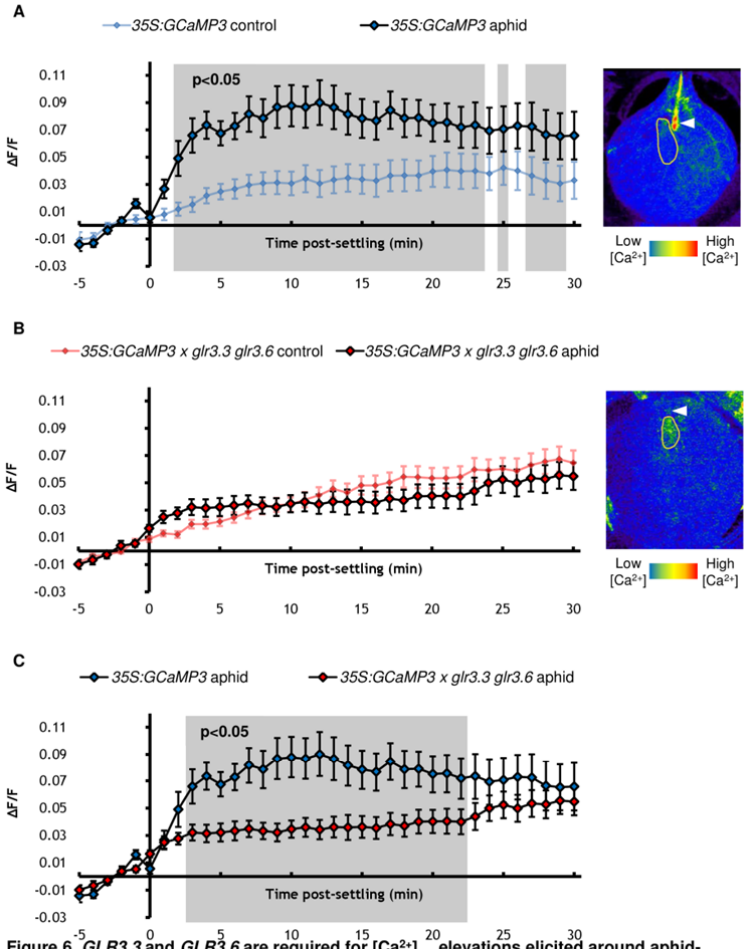

Figure 6. *GLR3.3* and *GLR3.6* are required for $[Ca^{2+}]_{cyt}$ elevations elicited around aphid-feeding sites.

A) Left: normalized fluorescence (ΔF/F) around feeding sites of *35S:GCaMP3* aphid-exposed leaves and no-aphid controls. Error bars represent SEM (n=34). Grey shading indicates significant difference between treatments (Student's t-test within GLM at p<0.05). Right: representative stereo-microscope image of the $[Ca^{2+}]_{cyt}$ elevations seen around an aphid-feeding of a *35S:GCaMP3* leaf. GFP fluorescence is colour-coded according to the inset scale. Aphid outlined in yellow and feeding site indicated with an arrowhead. Image taken at 3 min post-settling.

B) Left: ΔF/F around feeding sites of *35S:GCaMP3 x glr3.3 glr3.6* aphid-exposed leaves and no-aphid controls. Error bars represent SEM (n=37). Right: representative stereo-microscope image of the absence $[Ca^{2+}]_{cyt}$ elevation around an aphid-feeding site of a *35S:GCaMP3 x glr3.3 3.6* leaf. GFP fluorescence is colour-coded according to the inset scale. Aphid outlined in yellow and feeding site indicated with an arrowhead. Image taken at 3 min post-settling.

C) Comparison of ΔF/F around feeding sites of aphid-exposed *35S:GCaMP3* and *35S:GCaMP3 x glr3.3 glr3.6* leaves. Data of aphid exposures shown in panels A and B were replotted together. Areas shaded in grey indicate significant differences between the two treatments (Student's t-test within GLM at p<0.05).

259 feeding sites.

260

TPC1 contributes to the aphid-elicited $[Ca^{2+}]_{cyt}$ elevation

TPC1 has been implicated in Ca^{2+} signalling during insect attack, with local and systemic wound-induced Ca^{2+} signals lost in the *tpc1-2* mutant (Kiep et al., 2015). To assess whether *TPC1* plays a role in aphid-induced Ca^{2+} signalling, GCaMP3 was introduced into the *tpc1-2* mutant and the *35S:TPC1 5.6* over-expression line (Peiter et al., 2005). In comparison to *35S:GCaMP3* (Figure 7A), the $[Ca^{2+}]_{cyt}$ elevations around the aphid-feeding sites of *35S:GCaMP3* x *tpc1-2* leaves were significantly reduced, though not totally abolished (Figure 7B, Figure 7C, Supplemental Movie 7), implying that intracellular Ca^{2+} is involved in the $[Ca^{2+}]_{cyt}$ elevations. Overexpression of *TPC1* had no effect on the initial phases of $[Ca^{2+}]_{cyt}$ elevation, though the elevation was significantly extended beyond 25 min in a non-aphid-specific manner (Figure 8, Supplemental Movie 8).

Over-activation of TPC1 results in systemic $[Ca^{2+}]_{cyt}$ elevations and decreased aphid fecundity

Over-activation of TPC1 can be achieved via the *fatty acid oxygenation upregulated 2* (*fou2*) mutation that results in enhanced TPC1 channel opening (Bonaventure et al., 2007a). *35S:GCaMP3* x *fou2* leaves showed unchanged $[Ca^{2+}]_{cyt}$ elevations around *M. persicae* feeding sites (Figure 9A). However, $[Ca^{2+}]_{cyt}$ elevations in leaf tissue systemic to the aphid-feeding sites were detected and these elevations were significantly higher than those observed in *35S:GCaMP3* leaves (Figure 9B, Figure 9C, Supplemental Movie 9).

To determine whether the feeding site $[Ca^{2+}]_{cyt}$ elevation had an effect on aphid fitness, the number of progeny produced by *M. persicae* (fecundity) was

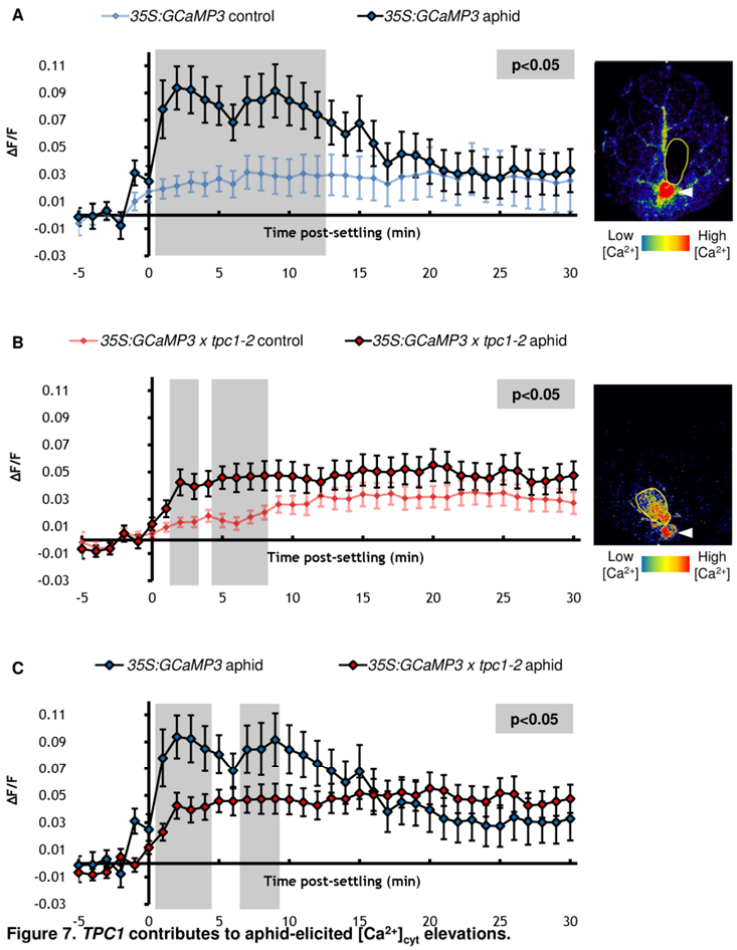

Figure 7. *TPC1* contributes to aphid-elicited $[Ca^{2+}]_{cyt}$ elevations.

A) Left: normalized fluorescence (ΔF/F) around feeding sites of aphid-exposed *35S:GCaMP3* leaves and no-aphid controls. Error bars represent SEM (n=27). Grey shading indicates significant difference between treatments (Student's t-test within GLM at p<0.05). Right: representative stereo-microscope image of the $[Ca^{2+}]_{cyt}$ elevation seen around a feeding site of a *35S:GCaMP3* leaf. GFP fluorescence is colour-coded according to the inset scale. Aphid outlined in yellow and feeding site indicated with an arrowhead. Image taken 1 min post-settling.

B) Left: ΔF/F around feeding sites of aphid-exposed *35S:GCaMP3 x tpc1-2* leaves and no-aphid controls. Error bars represent SEM (n=29). Grey shaded areas indicate significant differences between the two treatments (Student's t-test within GLM at p<0.05). Right: representative stereo-microscope image of the reduction in $[Ca^{2+}]_{cyt}$ elevation seen around a feeding site of a *35S:GCaMP3 x tpc1-2* leaf. GFP fluorescence is colour-coded according to the inset scale. Aphid outlined in yellow and feeding site indicated with an arrowhead. Image taken 2 min post-settling.

C) Comparison of ΔF/F around feeding sites of aphid-exposed *35S:GCaMP3* and *35S:GCaMP3 x tpc1-2* leaves. Data of aphid exposures shown in panels A and B were replotted together. Areas shaded in grey indicate significant differences between the two treatments (Student's t-test within GLM at p<0.05).

286 assessed. *M. persicae* fecundity was unaltered on the *glr3.3 glr3.6* mutant (Figure
287 10A) the *tpc1-2* mutant (Figure 10B) and the *35S:TPC1 5.6* line (Figure 10C). *M.*

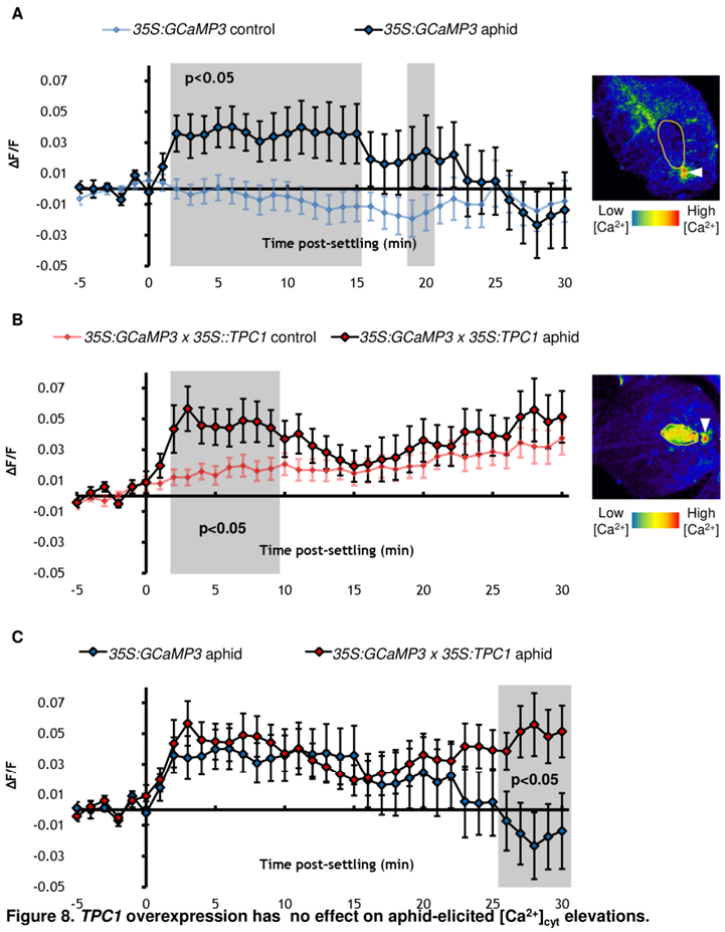

Figure 8. *TPC1* overexpression has no effect on aphid-elicited $[Ca^{2+}]_{cyt}$ elevations.

A) Left: normalized fluorescence (ΔF/F) around feeding sites of aphid-exposed *35S:GCaMP3* leaves and no-aphid controls. Error bars represent SEM (n=30). Grey shading indicates significant difference between treatments (Student's t-test within GLM at p<0.05). Right: representative stereo-microscope image of the $[Ca^{2+}]_{cyt}$ elevation seen around a feeding site of a *35S:GCaMP3* leaf. GFP fluorescence is colour-coded according to the inset scale. Aphid outlined in yellow and feeding site indicated with an arrowhead. Image taken 6 min post-settling.

B) Left: ΔF/F around feeding sites of aphid-exposed *35S:GCaMP3 x 35S:TPC1 5.6* leaves and no-aphid controls. Error bars represent SEM (n=29). Grey shaded areas indicate significant differences between the two treatments (Student's t-test within GLM at p<0.05). Right: representative stereo-microscope of the $[Ca^{2+}]_{cyt}$ elevation seen around a feeding site of a *35S:GCaMP3 x 35S:TPC1 5.6* leaf. GFP fluorescence is colour-coded according to the inset scale. Aphid outlined in yellow and feeding site indicated with an arrowhead. Image taken 5 min post-settling.

C) Comparison of ΔF/F around feeding sites of aphid-exposed *35S:GCaMP3* and *35S:GCaMP3 x 35S:TPC1 5.6* leaves. Data of aphid exposures shown in panels A and B were replotted together. Areas shaded in grey indicate significant differences between the two treatments (Student's t-test within GLM at p<0.05).

288 *persicae* fecundity on the *bak1-5* mutant has been assessed previously and is also
289 not significantly different from wild type (Prince et al., 2014). However, the *fou2*

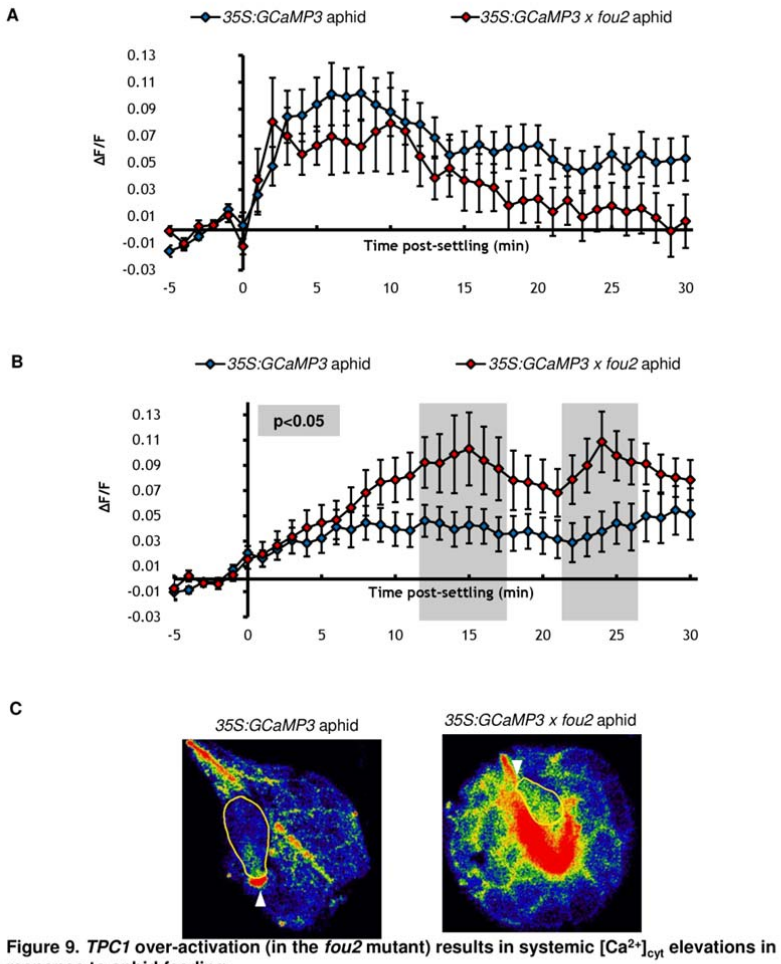

Figure 9. *TPC1* over-activation (in the *fou2* mutant) results in systemic $[Ca^{2+}]_{cyt}$ elevations in response to aphid feeding.

A) Comparison of normalized fluorescence (ΔF/F) around feeding sites of aphid-exposed *35S:GCaMP3* and aphid-exposed *35S:GCaMP3* x *fou2* leaves. Error bars represent SEM (*35S:GCaMP3* n=28, *35S:GCaMP3 x fou2* n=25).

B) Comparison of ΔF/F around systemic lateral tissue sites of aphid-exposed *35S:GCaMP3* and aphid-exposed *35S:GCaMP3* x *fou2* leaves. Error bars represent SEM (*35S:GCaMP3* n=28, *35S:GCaMP3 x fou2* n=25). Grey shading indicates significant difference between treatments (Student's t-test within GLM at p<0.05).

C) Representative stereo-microscope images of the $[Ca^{2+}]_{cyt}$ elevations seen in *35S:GCaMP3* (left) *35S:GCaMP3* x *fou2* (right) leaves exposed to *M. persicae*. GFP fluorescence is colour-coded according to the inset scale. Aphid outlined in yellow and feeding site indicated with an arrowhead. Image on left taken at 2 min post-settling, image on right taken at 10 min post-settling.

290 mutation resulted in a significant reduction in *M. persicae* fecundity (Figure 10D).
291 Interestingly, when the *fou2* mutant was crossed with the jasmonic acid (JA)

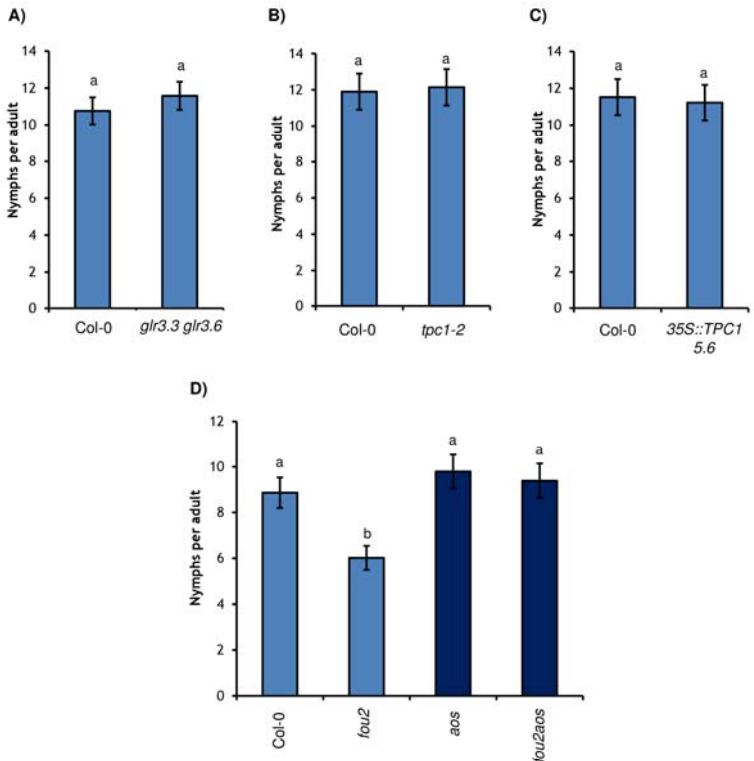

Figure 10. Aphid fecundity is reduced by TPC1 over-activation (*fou2*), but not by altering the expression of *TPC1* or abolishing transcription of *GLR3.3/3.6.*
M. persicae fecundity quantified by the total number of progeny produced per adult over 14 days. Letters indicate significant difference between genotypes (Student's t-test within GLM, $p<0.05$).

A) Fecundity is not altered on the *glr3.3 glr3.6* mutant . Bars represent SEM (n=24).

B) Fecundity is not altered on the *tpc1-2* mutant. Bars represent SEM (n=12).

C) Fecundity is not altered on the *35S:TCP1 5.6* line. Bars represent SEM (n=12).

D) Fecundity is significantly reduced on the *fou2* mutant, and can be rescued on the *fou2 aos* double mutant. Bars represent SEM (n=16).
Please remove the background lines in the graphs.
Please update the names on the figure (and check this in all figures).

292 synthesis mutant *allene oxide synthase* (*aos*) (Park et al., 2002), the *M. persicae*
293 fecundity was similar to that of wild-type plants (Figure 10D), indicating that the

documented increase in JA synthesis in the *fou2* mutant (Bonaventure et al., 2007a) is responsible for the decline in *M. persicae* fecundity. Aphid feeding behaviour was also assessed using EPG on the *bak1-5*, *tpc1-2* and *35S:TPC1 5.6* lines (Supplemental Data Set 1), with few differences found between genotypes.

DISCUSSION

To date, the majority of studies dissecting the genetic components involved in plant biotic $[Ca^{2+}]_{cyt}$ elevations have been conducted by application of elicitors to leaf sections, wounding of leaves via tweezers or application of chewing insects - all treatments that typically involve exposure of large number of cells to elicitation. Here, we elucidated the genetic components involved in $[Ca^{2+}]_{cyt}$ elevations upon plant perception of a piercing-sucking insect that attacks only a small number of epidermal and mesophyll cells within a leaf, as outlined in Figure 11. Aphids trigger $[Ca^{2+}]_{cyt}$ elevations during probing of epidermal and mesophyll cells. These $[Ca^{2+}]_{cyt}$ elevations are dependent on *BAK1* and *GLR3.3/GLR3.6*, which are key regulators of PTI and import of extracellular Ca^{2+} into the plant cell cytoplasm, respectively (Chinchilla et al., 2007; Tapken and Hollmann, 2008; Vincill et al., 2012). Furthermore, this study has revealed the role of an endomembrane channel, TPC1, in this interaction and provides evidence for the role of TPC1 in Ca^{2+}-induced Ca^{2+} release (Allen and Sanders, 1996; Ward and Schroeder, 1994). In accord with this interpretation, $[Ca^{2+}]_{cyt}$ elevations were amplified in the *fou2* mutant, which has an overactive TPC1 channel (Bonaventure et al., 2007a; Bonaventure et al., 2007b), and this resulted in *M. persicae* producing less progeny, implying that TPC1 plays a role in plant immunity.

The dependence of the aphid-elicited $[Ca^{2+}]_{cyt}$ elevation on *BAK1* clearly demonstrates that this response forms part of PTI. Whilst wounding during herbivory by chewing insects is sufficient to induce Ca^{2+} signalling (Maffei et al., 2004; Yang et al., 2012; Kiep et al., 2015), aphids probe only a small number of cells (Will and van Bel, 2006), and thus are more comparable to microbial pathogens. Indeed, *BAK1* is

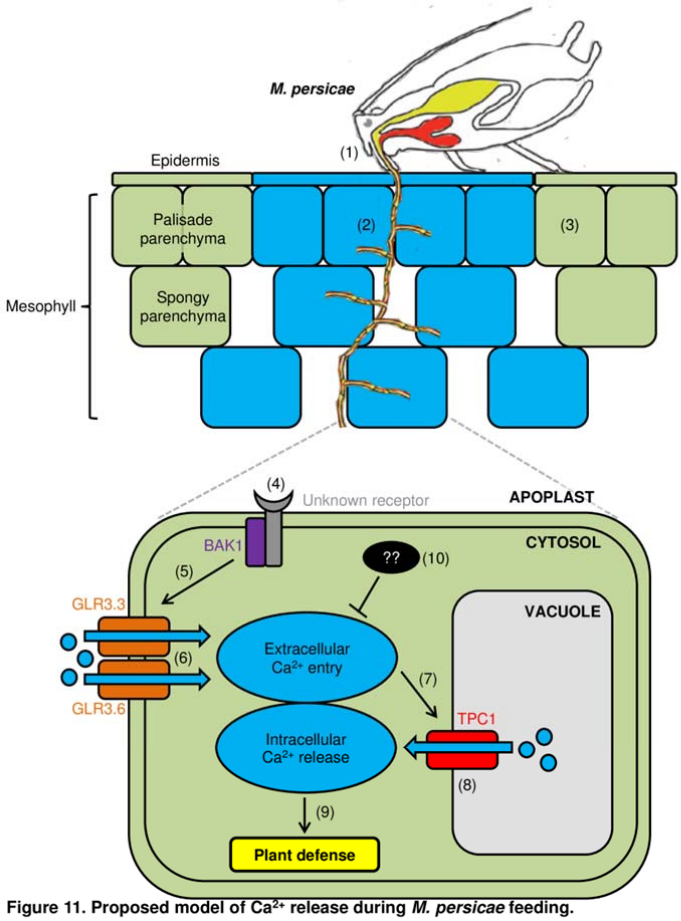

Figure 11. Proposed model of Ca^{2+} release during *M. persicae* feeding.

Aphid image taken from Hogenhout and Bos (2011). (1) Aphids typically probe epidermal and mesophyll cell layers within 31 s of the start of feeding. (2) An aphid-induced $[Ca^{2+}]_{cyt}$ elevation can be detected around the feeding site within 95 s of settling that spreads to adjacent cells. (3) This $[Ca^{2+}]_{cyt}$ elevation is not detected systemically beyond the feeding site. (4) BAK1 and an unknown receptor (PRR) perceive aphid herbivore-associated molecular patterns (HAMPs) (Prince et al., 2014). (5) Perception of aphid HAMPs by BAK1 leads to activation of GLR3.3/GLR3.6, potentially through the release of glutamate (Chiu et al., 2002, Qi et al., 2006, Forde and Lea, 2007, Stephens et al., 2008). (6) GLR3.3/GLR3.6 mediate extracellular Ca^{2+} influx into the cell (Tapken and Hollmann, 2008, Vincill et al., 2012). (7) The increase in $[Ca^{2+}]_{cyt}$ results in activation of TPC1 (Hedrich and Neher, 1987, Ward and Schroeder, 1994). (8) TPC1, either directly or indirectly mediates release of intracellular Ca^{2+} from the vacuole (Peiter et al., 2005). (9) The increase in $[Ca^{2+}]_{cyt}$ may result in the activation of plant immunity against aphids, which can be enhanced by over-activation of TPC1. (10) During compatible interactions, such as that between Arabidopsis and *M.* persicae, the aphid supresses plant immunity using effectors (Bos et al., 2010, Mugford et al., 2016), which might also supresses $[Ca^{2+}]_{cyt}$ elevations.

325 an essential component of PTI against microbial pathogens (Chinchilla et al., 2007;
326 Heese et al., 2007) and aphids (Prince et al., 2014; Chaudhary et al., 2014). Several

plasma membrane PRRs that interact with *BAK1* have been implicated in Ca^{2+} release during plant-microbe interactions, including CERK1, FLS2, EFR, and PEPR1 (Miya et al., 2007; Jeworutzki et al., 2010; Qi et al., 2010; Ma et al., 2012). Elicitors that are detected by such PRRs, including chitin, flg22, elf18 and Pep3 all induce rapid $[Ca^{2+}]_{cyt}$ elevations in Arabidopsis leaves within 2-3 mins (Ranf et al., 2008; Ma et al., 2012; Keinath et al., 2015), comparable to the rapid elevations seen in response to aphid feeding. Whilst GroEL from the aphid endosymbiont *Buchnera aphidicola* has been identified as the aphid elicitor of BAK1-mediated PTI (Chaudhary et al., 2014), CERK1, FLS2, EFR and PEPR1 are not involved (Prince et al., 2014). Our study provides direct, *in vivo* evidence of the involvement of BAK1 in PTI $[Ca^{2+}]_{cyt}$ elevations that are unlikely to be the result of wounding, and implicates the involvement of an as-yet unknown PRR in mediating these elevations.

Plant $[Ca^{2+}]_{cyt}$ elevations are observed in a larger area than the small number of cells directly probed by the aphid stylets (Tjallingii, 1985; Tjallingii and Esch, 1993) and can be detected within 95 s of aphid settling, suggesting that $[Ca^{2+}]_{cyt}$ elevations spread within the epidermal and mesophyll cells upon perception of aphid feeding. However, the highly localised spread of the feeding site $[Ca^{2+}]_{cyt}$ elevation in the epidermal and mesophyll cells is significantly different from the systemic, phloem-based signals seen in response to wounding and herbivory (Mousavi et al., 2013; Kiep et al., 2015). In addition, the 6 μm/s speed of the Ca^{2+} spread is significantly slower than the systemically-propagating Ca^{2+} signals in roots during salt stress, or the electrical signals within leaves during wounding, both of which travel at around 400 μm/s (Choi et al., 2014; Mousavi et al., 2013). Indeed, a phloem-based signal is required for systemic spread (Mousavi et al., 2013; Kiep et al., 2015), and this might

352 explain the lack of long-distance systemic $[Ca^{2+}]_{cyt}$ elevations in response to aphids.
353 Agreeing with this, *M. persicae* feeding fails to prime systemic defences in
354 Arabidopsis (Zhang et al., 2015), unlike microbial pathogens (Traw et al., 2007;
355 Conrath, 2011). This lack of response suggests that the aphid might be actively
356 supressing systemic signalling, as seen with caterpillars (Kiep et al., 2015). Taken
357 together, our data describe a $[Ca^{2+}]_{cyt}$ elevation that spreads outside of the phloem,
358 in the epidermal and mesophyll cells upon perception of a biotic threat.
359
360 *GLR3.3* and *GLR 3.6* are also required for the aphid-elicited $[Ca^{2+}]_{cyt}$
361 elevations to occur, establishing the apoplast as a source of the Ca^{2+} released
362 during detrimental biotic interactions. An influx of Ca^{2+} from the extracellular space
363 can be observed during plant-microbe interactions (Gelli et al., 1997; Blume et al.,
364 2000) that can be blocked by plasma membrane channel inhibitors (Zimmermann et
365 al., 1997; Lecourieux et al., 2002; Lecourieux et al., 2005). In addition, a net Ca^{2+}
366 efflux from the extracellular space of tobacco leaf disks was recently measured after
367 *M. persicae* feeding using Ca^{2+}-selective microelectrodes (Ren et al., 2014). *GLR3.3*
368 and *GLR3.6* have been implicated in systemic electrical signalling during wounding
369 (Mousavi et al., 2013; Salvador-Recatala, 2016), and *GLR3.3* regulates damage
370 perception during oomycete infection (Manzoor et al., 2013). However, given the
371 involvement of *BAK1* in the *M. persicae*-induced $[Ca^{2+}]_{cyt}$ elevation, it is likely that the
372 GLRs are acting as a part of PTI during plant-aphid interactions. Indeed, GLRs have
373 been implicated in PAMP perception, with iGluR (mammalian GLR homologues)
374 inhibitors attenuating flg22- elf18- and chitin-induced $[Ca^{2+}]_{cyt}$ elevations (Kwaaitaal
375 et al., 2011). Interestingly, it is possible that glutamate itself is a GLR-activating
376 ligand (Chiu et al., 2002; Qi et al., 2006; Forde and Lea, 2007; Stephens et al.,

2008). The fungal PAMP cryptogein can elicit an extracellular rise in glutamate and $[Ca^{2+}]_{cyt}$ that is driven by exocytosis (Vatsa et al., 2011), suggesting that glutamate release from the cell is downstream of PAMP perception (Weiland et al., 2016). This might provide a mechanism by which BAK1-mediated glutamate release could stimulate GLR activation. However, to our knowledge no direct link between BAK1 and glutamate release has yet been established. Our current findings demonstrate a role for the GLRs in local Ca^{2+} signalling and directly identify GLRs as a mechanism leading to of $[Ca^{2+}]_{cyt}$ elevations during biotic interactions.

A long-standing question regarding Ca^{2+} signalling in plants relates to the way in which various Ca^{2+} release pathways interact to produce stimulus-specific signatures. The nature of the interplay of plasma membrane and endomembrane Ca^{2+} release channels has been particularly opaque. It has been hypothesised that *TPC1*, which mediates release of Ca^{2+} from the lumen of the vacuole into the cell cytoplasm (Ward and Schroeder, 1994; Peiter et al., 2005), contributes to Ca^{2+}-induced Ca^{2+} release (Ward and Schroeder, 1994; Allen and Sanders, 1996). Since the feeding site $[Ca^{2+}]_{cyt}$ elevations are attenuated, but not abolished in the *tpc1-2* mutant, it appears that release of vacuolar Ca^{2+} by *TPC1* is downstream of and dependent on extracellular Ca^{2+} release by the GLRs. This finding agrees with work showing that TPC1 activity is positively regulated by $[Ca^{2+}]_{cyt}$ (Hedrich and Neher, 1987; Ward and Schroeder, 1994; Allen and Sanders, 1996; Guo et al., 2016; Kintzer and Stroud, 2016) and plays a role in systemically-propagating Ca^{2+}-induced Ca^{2+} release (Dubiella et al., 2013; Evans et al., 2016; Gilroy et al., 2016; Choi et al., 2016). Consequently, TPC1 appears to be activated by GLR-mediated Ca^{2+} influx and involved in the cell-to-cell spread of Ca^{2+} during biotic interactions. Moreover,

mature sieve elements do not contain vacuoles (Esau, 1977), supporting our conclusion that the $[Ca^{2+}]_{cyt}$ elevations do not occur in the phloem, and Arabidopsis spongy mesophyll cells contain a higher $[Ca^{2+}]_{vac}$ than most other cell types (Conn et al., 2011a; Conn et al., 2011b), making them a significant source of Ca^{2+} influx. Importantly, mesophyll $[Ca^{2+}]_{vac}$ is not significantly altered in *tpc1-2* (Gilliham et al., 2011) and consequently the reduced Ca^{2+} burst in the *tpc1-2* mutant is not related to reduced vacuolar storage of Ca^{2+}. Thus, we have identified a role for *TPC1* in Ca^{2+}-induced Ca^{2+} release during biotic interactions, contributing to the growing body of evidence demonstrating the biological relevance of this channel in plants.

Despite the role of *BAK1*, *GLR3.3*, *GLR3.6*, and *TPC1* in generating the aphid-elicited $[Ca^{2+}]_{cyt}$ elevations and the established role of BAK1 and Ca^{2+} in PTI (Blume et al., 2000; Lecourieux et al., 2005; Keinath et al., 2015), abolishing transcription of these genes had no effect on *M. persicae* performance. Downstream of aphid perception by BAK1, hallmarks of PTI such as ROS production, callose deposition, and the expression of defence marker genes occur (Prince et al., 2014; Chaudhary et al., 2014). Furthermore, *BAK1* is required for plants to prime defence against *M. persicae* after prior exposure to aphids (Prince et al., 2014). Despite this, *M. persicae* fecundity is unaltered on the *bak1-5* mutant (Prince et al., 2014), as seen for the *glr3.3 glr3.6* or *tpc1-2* mutants in this study. Aphid feeding behaviour was also largely unaltered on the *bak1-5* and *tpc1-2* mutants, indicating that the differences in the $[Ca^{2+}]_{cyt}$ elevations observed in these mutants was not the result of altered feeding behaviour. We therefore suggest that since *M. persicae* can feed successfully from Arabidopsis, plant immunity is already being sufficiently supressed. As a result, there is no capacity to increase plant susceptibility to the aphid by

disrupting Ca^{2+} signalling. The suppression of Arabidopsis defence by aphids is achieved via effector proteins (Bos et al., 2010; Hogenhout and Bos, 2011; Pitino and Hogenhout, 2013; Atamian et al., 2013; Elzinga et al., 2014; Naessens et al., 2015; Wang et al., 2015; Kettles and Kaloshian, 2016) that are injected into epidermal and mesophyll cells during feeding (Martin et al., 1997; Moreno et al., 2011; Mugford et al., 2016). These effectors may actively supress the feeding site $[Ca^{2+}]_{cyt}$ elevations, as aphid saliva contains Ca^{2+} binding proteins (Will et al., 2007; Carolan et al., 2009; Rao et al., 2013). Accordingly, the $[Ca^{2+}]_{cyt}$ elevations observed in response to *M. persicae* are not sufficient to activate additional defence, adding to a growing body of evidence showing that this insect is a highly adapted plant pest.

In agreement with the hypothesis that Ca^{2+} signalling forms part of the plant defence response, which *M. persicae* may be suppressing, enhancement of the feeding site $[Ca^{2+}]_{cyt}$ elevations was detrimental to the aphids. Over-activation of *TPC1* via the *fou2* mutation resulted in the generation of systemic $[Ca^{2+}]_{cyt}$ signals not seen in wild-type plants, and significantly reduced aphid fecundity. These observations fit with the understanding that TPC1 is regulated post-transcriptionally (Gfeller et al., 2011) and is involved in systemic Ca^{2+} signalling (Choi et al., 2014; Kiep et al., 2015), and that the *fou2* mutation is detrimental to the specialist aphid *Brevicoryne brassicae* (Kusnierczyk et al., 2011). Given the lack of a phenotype in the *TPC1* overexpression line, these data also imply that the voltage sensitivity of TPC1 is more important than protein abundance in biotic interactions. Furthermore, this result suggests that *in vivo* there is a role for changes in the trans-tonoplast voltage to regulate vacuolar Ca^{2+} release and aphid defence responses. The detrimental effect of the *fou2* mutation on *M. persicae* was dependent on JA

452 production by *AOS*, in accord with the upregulation of JA and JA-related transcripts
453 in the *fou2* mutant (Bonaventure et al., 2007a; Bonaventure et al., 2007b). The
454 involvement of JA in aphid–plant interactions is unclear, with some reporting an
455 effect of JA on aphids (Ellis et al., 2002) and others not (Staswick et al., 1992;
456 Kusnierczyk et al., 2011; Kettles et al., 2013). Furthermore, the activation of systemic
457 $[Ca^{2+}]_{cyt}$ elevations in the *fou2* mutant suggests that systemic spread of the signal via
458 Ca^{2+}-induced Ca^{2+} release might lead to activation of defence, and that aphid
459 suppression of this is based on restricting these signals to a small area. Thus, our
460 data suggest that over-activation of Ca^{2+} signalling is a potential mechanism by
461 which to increase plant resistance to pests.
462
463

464

METHODS

Arabidopsis growth

Plants used in the microscopy and single leaf EPG were grown on 100 mm^2 square plastic plates (R & L Slaughter Ltd, Upminster, UK) on ¼ strength Murashige and Skoog (MS) medium (recipe: 1.1 g Murashige and Skoog medium, 7.5 g sucrose, 10 g Formedium agar, 1 L de-ionised water) (Murashige and Skoog, 1962) and stratified for three days in the dark (8°C). They were then transferred to a controlled environment room (CER) with a 16 h day and 8 h night (90 µmol m^{-2} s^{-1} sodium lamp), at a constant temperature of 23°C. Plants were used in experiments at 16-18 days old. Plants for use in fecundity assays and whole-plant EPG were germinated and maintained on Scotts Levington F2 compost (Scotts, Ipswich, UK). Seeds were stratified for one week at 4–6°C before being transferred to a CER for 4–5 weeks, maintained at 22°C and with a photoperiod of 10 h light (90 µmol m^{-2} s^{-1} sodium lamp) and 14 h dark.

Aphids

A stock colony of *M. persicae* (clone US1L, Mark Stevens, Brooms Barn) (Bos et al., 2010) was reared continuously on Chinese cabbage (*Brassica rapa,* subspecies *chinensis*) in cages in a 16 h day (90 µmol m^{-2} s^{-1} at 22°C), 8 h night (20°C) photoperiod. For use in experiments, *M. persicae* individuals of standardized ages were used. These were produced by placing 5-15 mixed instar adults from the stock colony onto four-week-old Arabidopsis (Col-0) grown in a CER with a 16 h day (90 µmol m^{-2} s^{-1} at 22°C) and 9 h night (20°C) photoperiod, in pots (13.5 cm diameter, 9 cm depth) and caged inside clear plastic tubing (10 cm x 15 cm) with a

plastic lid. These adults were removed after 24–48 h, leaving nymphs of the same age for use in later experiments.

Fluorescence microscopy

Leaves from plate-grown plants were detached using sharp scissors, and placed in the wells of a clear 96-well Microtitre™ plate (ThermoFisher Scientific) with 300 µL of distilled water, abaxial surface facing up. These plates were left in the dark at room temperature overnight and used in microscopy the following day. To visualise fluorescence from the *35S:GCaMP3* construct (Kd *in vitro* = 660 ±19 nM, Tian et al., 2009), a Leica M205FA stereo microscope (Leica Microsystems) was used. GFP was excited using a LED light source at 470 nm and fluorescent emission was captured using a 500 - 550 nm emission filter. Images were captured every 5 seconds using a Leica DFC310FX camera with a gain of 3.5 and a constant exposure time (1–2.5 seconds depending on the brightness of the line). The microscope was controlled via Leica Application Suite v3.2.0 (Leica Microsystems). Leaves were imaged in groups of four, two leaves per genotype, at a 7.8 X magnification. One 8–10-day-old aphid was added to a leaf of each genotype, with the other leaf left un-infested as a control. Each leaf represented one biological replicate (n). Images were captured for 50–60 min after aphid application, with the 96-well plate covered in cling film to prevent aphid escape. Images were exported as Tagged Image File Format (TIFF) files for analysis.

Fluorescent signal analysis

TIFF files were imported into Fiji (Image J) v1.48a (National Institutes of Health, USA) and converted into 32-bit images. Fluorescence was analysed over time for various regions of interest (ROIs) using the Fiji plugin Time Series Analyser v2 (University of California, Los Angeles, CA, USA). For aphid treatments, circular ROIs with a 50 pixel (0.65 mm) diameter were selected in three locations: at the feeding site, on the midrib systemic to the aphid feeding site, and in the tissue beside the midrib ('lateral tissue'). $\Delta F/F$ was calculated according to the equation $\Delta F/F = (F - F_0)/F_0$, where F_0 was the average baseline fluorescence calculated from the average of F over the first 60 frames of the recording (Keinath et al., 2015) before the aphid settled. Samples in which the controls showed large $[Ca^{2+}]_{cyt}$ elevations ($\Delta F/F > 0.2$) prior to treatment were discarded. The area of the aphid-elicited $[Ca^{2+}]_{cyt}$ elevations was calculated using the Fiji freehand selection tool to draw around the maximum visible GFP signal. For analysis of the speed of the wave front, the Fiji plugin MTrackJ v 1.5.1 (Meijering et al., 2012) was used. Representative supplemental videos of the aphid-elicited $[Ca^{2+}]_{cyt}$ elevations were created by converting the raw F values to heat maps using the NucMed_Image LUTs plugin for Fiji (J.A. Parker, IEEE.org), with the feeding site Ca^{2+} burst used to determine the colour scale. Time information was added using the Time Stamper plugin (W. Rasband, National Institutes of Health, USA).

Confocal Microscopy

Confocal images of the GCaMP3 signal were acquired with a laser scanning confocal microscope (LSM780/Elyra, Newcomb Imaging Center, Department of Botany, UW-Madison). GCaMP3 was excited by a 488 nm laser and GFP signal was detected with a 34 element internal GAsP detector.

Crossing Arabidopsis

Crossing was conducted with 4-week-old Arabidopsis plants, grown in a CER at a constant temperature of 22°C with a 16 h day (HQI lighting), 8 h night photoperiod. Two unopened buds per stalk were selected and the remaining buds were removed. The sepals, petals and stamens were removed from the selected buds, leaving a single carpel. Stamens from the other crossing partner were dissected and pollen transfer between the two was achieved by brushing the stamen against the carpel of the selected mutant. Dissections were carried out with a pair of sharp tweezers. Pollinated carpels were covered in 74 mm x 41 mm paper bags (Global Polythene, Preston, UK) sealed with tape and allowed to mature.

Whole-plant EPG

Experiments were conducted as described previously (Tjallingii, 1978). Adult 13-15 day old *M. persicae* were attached to the Giga-8 EPG system (EPG Systems, Wageningen, Netherlands) using 12.5 µm gold wire (EPG Systems) and silver glue (EPG Systems) and then placed on 4-week old Arabidopsis. One aphid was added to each plant and this represented one biological replicate (n). The experiment was contained inside a Faraday cage to minimise electrical interference. Feeding behaviour was recorded for 8 h using Stylet+d (EPG Systems). Each EPG track was then analysed blind in Stylet+a (EPG Systems). The timing of aphid settling relative to the beginning of probing was also documented. Relevant EPG parameters were calculated using the Microsoft Excel spreadsheet developed by Dr Edgar Schliephake (Julius Kuhn Institute, Germany) (Sarria et al., 2009).

562 **Single-leaf EPG**

563 Single-leaf EPG was performed using a modified version of the set-up
564 described above. Leaves were dissected from plate-grown plants (grown as detailed
565 the microscopy section) and floated in 300 µL of water in 96-well plates. A small
566 piece of copper wire was attached to the EPG ground electrode, and this was
567 inserted into the well. Nine-to-eleven-day-old *M. persicae* were then added to these
568 leaves and the experiment was conducted and analysed as outlined above.

569

570 **Aphid fecundity assay**

571 *M. persicae* fecundity was assessed as previously described (Pitino et al.,
572 2011). Briefly, five adult aphids from the stock colony were added to each plant at
573 the beginning of the experiment, and after 48 h all adults were removed. After a
574 further 72 h, any excess nymphs were removed, to leave five nymphs per plant. The
575 number of offspring produced by these aphids was counted after 11 and 14 days, as
576 was the final number of adult aphids. Each plant was considered one biological
577 replicate (n).

578

579 **Statistical analysis**

580 Genstat v18 (VSN International) was used for the majority of statistical
581 analyses. GCaMP3 fluorescence data were assessed using classical linear
582 regression within a General Linear Model (GLM). Pairwise comparisons between
583 treatments at each time point were conducted within this model using Student's t
584 probabilities. Aphid fecundity assays were analysed by a classical linear regression
585 within a GLM using a Poisson distribution. The model took into account the
586 experimental replicates as an additional factor. Pairwise comparisons between

587 treatments using Student's t probabilities were conducted within this model. EPG
588 data was analysed in R v3.0 (Free Software Foundation, Boston, MA, USA) by
589 comparing behaviours between treatments using a Mann-Whitney U test.
590
591 **Accession Numbers**
592 Sequence data from this article can be found in the Arabidopsis Genome Initiative or
593 GenBank/EMBL databases under the following accession numbers: ADJ53338.1
594 (GCaMP3), NC_003075.7 (Two-pore channel 1), NC_003075.7 **(**BRI1-associated
595 receptor kinase), NC_003070.9 (glutamate receptor 3.3), NC_003074.8 (glutamate
596 receptor 3.6), NC_003070.9 (sucrose-proton symporter 2), and NC_003076.8 (allene
597 oxide synthase).
598
599 **Supplemental Data**
600 **Supplemental Figure 1 (Supports Figure 1).** GCaMP3 sub-cellular localization in
601 the epidermis of *35S:GCaMP3* leaves, measured by confocal microscopy.
602 **Supplemental Movie 1 (Supports Figure 1).** The GCaMP3 sensor detects aphid-
603 elicited $[Ca^{2+}]_{cyt}$ elevations in detached leaves.
604 **Supplemental Movie 2 (Supports Figure 2).** The GCaMP3 sensor detects
605 [Ca2+]cyt elevations around the putative aphid feeding site on leaves of whole
606 Arabidopsis plants.
607 **Supplemental Movie 3 (Supports Figure 4).** $[Ca^{2+}]_{cyt}$ elevations are detected
608 around feeding sites of aphid-exposed *35S:GCaMP3* leaves, but not
609 *SUC2pro:GCaMP3* leaves.
610 **Supplemental Movie 4 (Supports Figure 4).** Visualisation of $[Ca^{2+}]_{cyt}$ elevations
611 elicited by cold water on *35S:GCaMP3* and *SUC2pro:GCaMP3* leaves.

612 **Supplemental Movie 5 (Supports Figure 5).** *BAK1* is required for $[Ca^{2+}]_{cyt}$

613 elevations elicited around aphid-feeding sites.

614 **Supplemental Movie 6 (Supports Figure 6).** *GLR3.3* and *GLR3.6* are required for

615 $[Ca^{2+}]_{cyt}$ elevations elicited around aphid-feeding sites.

616 **Supplemental Movie 7 (Supports Figure 7).** *TPC1* contributes to aphid-elicited
617 $[Ca^{2+}]_{cyt}$ elevations.

618 **Supplemental Movie 8(Supports Figure 8).** Aphid-induced $[Ca^{2+}]_{cyt}$ elevations are

619 not altered by overexpression of *TPC1.*

620 **Supplemental Movie 9 (Supports Figure 9).** Over-activation of TPC1 results in

621 systemic aphid-elicited $[Ca^{2+}]_{cyt}$ elevations.

622 **Supplemental Data Set 1 (Supports Figure 3).** Aphid feeding behaviors analyzed

623 by EPG on selected Arabidopsis mutants (pairwise comparisons).

624

625

ACKNOWLEDGEMENTS

We would like to thank Grant Calder (John Innes Centre, U.K.) and W. Fred Tjallingii (EPG Systems, The Netherlands) for their invaluable advice concerning microscopy and EPG, respectively. The authors also wish to thank Edward Farmer (University of Lausanne, Switzerland) for plant material and the members of the John Innes Centre horticultural and entomology departments for their assistance throughout the project. This work was supported by a PhD studentship from the John Innes Foundation (T.V.), grant B/JJ004561/1 from the BBSRC and the John Innes Foundation (T.V., M.A., J.C., P.H., N.B., S.T.M., M.P., S.H., T.M., D.S.), a year in industry placement from the John Innes Centre (M.A.), a summer studentship from Biochemical Society of the UK (J.C.), JST PRESTO (M.T.) and grants MCB 1329723 and IOS-1557899 from the National Science Foundation (M.T., S.G.). The authors have no conflicts of interest to declare.

AUTHOR CONTRIBUTIONS

T.V., S.T.M, T.M., S.H. and D.S. designed the research. T.V., M.A., J.C., P.H., N.B. and M.P. performed experiments. M.T. and S.G. contributed new experimental tools and materials. T.V., M.A., J.C., P.H, N.B. and M.P. analysed results. T.V., S.G., T.M., S.H. and D.S wrote the paper.

FIGURE LEGENDS

Figure 1. The GCaMP3 sensor detects $[Ca^{2+}]_{cyt}$ elevations around the aphid feeding site on detached leaves.

A) Representative stereo-microscope images showing GFP fluorescence (colour coded according to the inset scale) around feeding sites of leaves exposed to a *M. persicae* adult at several time points after aphid settling. Aphid outlined in yellow. Location of feeding site indicated with an arrowhead.

B) Left: stereo-microscope image of a feeding site region (yellow circle) used for the analyses shown on the right (scale bar = 1 mm). Aphid outlined in yellow and location of feeding site indicated with an arrowhead. Right: normalised GFP fluorescence ($\Delta F/F$) measurements every 5 s around the feeding site from 5 min before until 10 min after settling of an adult aphid. F, average fluorescence intensity prior to aphid settling (baseline); ΔF, difference between measured fluorescence and baseline fluorescence. Error bars represent the standard error of the mean (SEM, n=34). The average area of the $[Ca^{2+}]_{cyt}$ elevation was 110±18 μm^2 and the leading wave front of this elevation travelled radially at 5.9 ±0.6 µm/s from its centre. Grey shading indicates a significant difference between treatments using a Student's t-test within a general linear model (GLM) at $p<0.05$.

Figure 2. The GCaMP3 sensor does not detect $[Ca^{2+}]_{cyt}$ elevations systemic to the aphid-feeding site.

A) Left: stereo-microscope image of a leaf exposed to an aphid with the yellow circle indicating the midrib region systemic to the feeding site (arrowhead) of an aphid (outlined in yellow). Scale bar = 1 mm. Right: normalized fluorescence ($\Delta F/F$) at midrib regions systemic to the aphid feeding sites (as exemplified with the yellow circle in the image on the left) of *35S:GCaMP3* leaves exposed to *M. persicae* adults and no-aphid controls. Error bars represent SEM (n=34). Data from aphid responding leaves are not significantly different from controls (Student's t-test within a GLM, $p>0.05$).

B) Left: stereo-microscope image of a leaf exposed to an aphid with the yellow circle indicating the lateral tissue regions (next to the midrib) systemic to the feeding site (arrowhead) of an aphid (outlined in yellow). Right: $\Delta F/F$ at lateral tissue regions systemic to the aphid-feeding sites (as exemplified with the yellow circle in the image on the left) of *35S:GCaMP3* leaves exposed to *M. persicae* adults and no-aphid controls. Error bars represent SEM (n=34). Data from aphid responding leaves are not significantly different from controls (Student's t-test within a GLM, $p>0.05$).

Figure 3. The pathway phase that includes aphid probing of epidermal and mesophyll cells starts immediately upon aphid settling.

Feeding phases represented by coloured shading.

A) Representative EPG trace from an aphid feeding on a whole Col-0 Arabidopsis plant. The first cell puncture occurred at 31 ± 11 s after the beginning of pathway phase, with the phloem accessed after 24 ± 3 min (n=22).

B) Representative EPG traces from aphids feeding on detached *35S:GCaMP3* leaves (n=6).

Figure 4. $[Ca^{2+}]_{cyt}$ elevations are not detected in the phloem around aphid feeding sites.

A) Left: normalized fluorescence ($\Delta F/F$) around aphid-feeding sites of *35S:GCaMP3* aphid-exposed leaves and no-aphid controls. Error bars represent SEM (n=31). Grey shading indicates significant difference between treatments (Student's t-test within GLM at $p<0.05$).

Right: representative stereo microscope image of a $[Ca^{2+}]_{cyt}$ elevation seen around an aphid-feeding site on a *35S:GCaMP3* leaf. GFP fluorescence is colour-coded according to the inset scale. Aphid outlined in yellow and feeding site indicated with an arrowhead. Image taken at 3 min post-settling.

B) Left: ΔF/F around the aphid-feeding sites of *SUC2pro:GCaMP3* aphid-exposed leaves and no-aphid controls. Error bars represent SEM (n=34). Right: representative stereo microscope image of the absence of $[Ca^{2+}]_{cyt}$ elevation around an aphid-feeding site on a *SUC2pro:GCaMP3* leaf. GFP fluorescence is colour-coded according to the inset scale. Aphid outlined in yellow and feeding site indicated with an arrowhead. Image taken at 3 min post-settling.

Figure 5. *BAK1* is required for eliciting $[Ca^{2+}]_{cyt}$ elevations around aphid-feeding sites.
A) Left: normalized fluorescence (ΔF/F) around feeding sites of *35S:GCaMP3* aphid-exposed leaves and no-aphid controls. Error bars represent SEM (n=30). Grey shading indicates significant difference between treatments (Student's t-test within GLM at $p<0.05$). Right: representative stereo-microscope image of the $[Ca^{2+}]_{cyt}$ elevation seen around an aphid-feeding site of a *35S:GCaMP3* leaf. GFP fluorescence colour-coded according to the inset scale. Aphid outlined in yellow and feeding site indicated with an arrowhead. Image taken at 2 min post-settling

B) Left: ΔF/F around feeding sites of *35S:GCaMP3 x bak1-5* aphid-exposed leaves and no-aphid controls. Error bars represent SEM (n=34). Right: representative stereo-microscope image of the absence of $[Ca^{2+}]_{cyt}$ elevation around an aphid-feeding site of a *35S:GCaMP3 x bak1-5* leaf. GFP fluorescence colour-coded according to the inset scale. Aphid outlined in yellow and feeding site indicated with an arrowhead. Image taken at 2 min post-settling.

C) Comparison of ΔF/F around feeding sites of aphid-exposed *35S:GCaMP3* and *35S:GCaMP3 x bak1-5* leaves. Data of aphid exposures shown in panels A and B were replotted together. Areas shaded in grey indicate significant differences between the two treatments (Student's t-test within GLM at $p<0.05$).

Figure 6. *GLR3.3* and *GLR3.6* are required for $[Ca^{2+}]_{cyt}$ elevations elicited around aphid-feeding sites.
A) Left: normalized fluorescence (ΔF/F) around feeding sites of *35S:GCaMP3* aphid-exposed leaves and no-aphid controls. Error bars represent SEM (n=34). Grey shading indicates significant difference between treatments (Student's t-test within GLM at $p<0.05$). Right: representative stereo-microscope image of the $[Ca^{2+}]_{cyt}$ elevations seen around an aphid-feeding of a *35S:GCaMP3* leaf. GFP fluorescence is colour-coded according to the inset scale. Aphid outlined in yellow and feeding site indicated with an arrowhead. Image taken at 3 min post-settling.

B) Left: ΔF/F around feeding sites of *35S:GCaMP3 x glr3.3 glr3.6* aphid-exposed leaves and no-aphid controls. Error bars represent SEM (n=37). Right: representative stereo-microscope image of the absence $[Ca^{2+}]_{cyt}$ elevation around an aphid-feeding site of a *35S:GCaMP3 x glr3.3 3.6* leaf. GFP fluorescence is colour-coded according to the inset scale. Aphid outlined in yellow and feeding site indicated with an arrowhead. Image taken at 3 min post-settling.

C) Comparison of ΔF/F around feeding sites of aphid-exposed *35S:GCaMP3* and *35S:GCaMP3 x glr3.3 glr3.6* leaves. Data of aphid exposures shown in panels A and B were replotted together. Areas shaded in grey indicate significant differences between the two treatments (Student's t-test within GLM at $p<0.05$).

Figure 7. *TPC1* contributes to aphid-elicited $[Ca^{2+}]_{cyt}$ elevations.
A) Left: normalized fluorescence (∆F/F) around feeding sites of aphid-exposed *35S:GCaMP3* leaves and no-aphid controls. Error bars represent SEM (n=27). Grey shading indicates significant difference between treatments (Student's t-test within GLM at p<0.05). Right: representative stereo-microscope image of the $[Ca^{2+}]_{cyt}$ elevation seen around a feeding site of a *35S:GCaMP3* leaf. GFP fluorescence is colour-coded according to the inset scale. Aphid outlined in yellow and feeding site indicated with an arrowhead. Image taken 1 min post-settling.

B) Left: ∆F/F around feeding sites of aphid-exposed *35S:GCaMP3 x tpc1-2* leaves and no-aphid controls. Error bars represent SEM (n=29). Grey shaded areas indicate significant differences between the two treatments (Student's t-test within GLM at p<0.05). Right: representative stereo-microscope image of the reduction in $[Ca^{2+}]_{cyt}$ elevation seen around a feeding site of a *35S:GCaMP3 x tpc1-2* leaf. GFP fluorescence is colour-coded according to the inset scale. Aphid outlined in yellow and feeding site indicated with an arrowhead. Image taken 2 min post-settling.

C) Comparison of ∆F/F around feeding sites of aphid-exposed *35S:GCaMP3* and *35S:GCaMP3 x tpc1-2* leaves. Data of aphid exposures shown in panels A and B were replotted together. Areas shaded in grey indicate significant differences between the two treatments (Student's t-test within GLM at p<0.05).

Figure 8. *TPC1* overexpression has no effect on aphid-elicited $[Ca^{2+}]_{cyt}$ elevations.
A) Left: normalized fluorescence (∆F/F) around feeding sites of aphid-exposed *35S:GCaMP3* leaves and no-aphid controls. Error bars represent SEM (n=30). Grey shading indicates significant difference between treatments (Student's t-test within GLM at p<0.05). Right: representative stereo-microscope image of the $[Ca^{2+}]_{cyt}$ elevation seen around a feeding site of a *35S:GCaMP3* leaf. GFP fluorescence is colour-coded according to the inset scale. Aphid outlined in yellow and feeding site indicated with an arrowhead. Image taken 6 min post-settling.

B) Left: ∆F/F around feeding sites of aphid-exposed *35S:GCaMP3 x 35S:TPC1 5.6* leaves and no-aphid controls. Error bars represent SEM (n=29). Grey shaded areas indicate significant differences between the two treatments (Student's t-test within GLM at p<0.05). Right: representative stereo-microscope of the $[Ca^{2+}]_{cyt}$ elevation seen around a feeding site of a *35S:GCaMP3 x 35S:TPC1 5.6* leaf. GFP fluorescence is colour-coded according to the inset scale. Aphid outlined in yellow and feeding site indicated with an arrowhead. Image taken 5 min post-settling.

C) Comparison of ∆F/F around feeding sites of aphid-exposed *35S:GCaMP3* and *35S:GCaMP3 x 35S:TPC1 5.6* leaves. Data of aphid exposures shown in panels A and B were replotted together. Areas shaded in grey indicate significant differences between the two treatments (Student's t-test within GLM at p<0.05).

Figure 9. *TPC1* over-activation (in the *fou2* mutant) results in systemic $[Ca^{2+}]_{cyt}$ elevations in response to aphid feeding.

A) Comparison of normalized fluorescence (∆F/F) around feeding sites of aphid-exposed *35S:GCaMP3* and aphid-exposed *35S:GCaMP3* x *fou2* leaves. Error bars represent SEM (*35S:GCaMP3* n=28, *35S:GCaMP3 x fou2* n=25).

B) Comparison of ΔF/F around systemic lateral tissue sites of aphid-exposed *35S:GCaMP3* and aphid-exposed *35S:GCaMP3* x *fou2* leaves. Error bars represent SEM (*35S:GCaMP3* n=28, *35S:GCaMP3 x fou2* n=25). Grey shading indicates significant difference between treatments (Student's t-test within GLM at $p<0.05$).

C) Representative stereo-microscope images of the $[Ca^{2+}]_{cyt}$ elevations seen in *35S:GCaMP3* (left) *35S:GCaMP3* x *fou2* (right) leaves exposed to *M. persicae*. GFP fluorescence is colour-coded according to the inset scale. Aphid outlined in yellow and feeding site indicated with an arrowhead. Image on left taken at 2 min post-settling, image on right taken at 10 min post-settling.

Figure 10. Aphid fecundity is reduced by TPC1 over-activation (*fou2*), but not by altering the expression of *TPC1* or abolishing transcription of *GLR3.3/3.6.*

M. persicae fecundity quantified by the total number of progeny produced per adult over 14 days. Letters indicate significant difference between genotypes (Student's t-test within GLM, $p<0.05$).

A) Fecundity is not altered on the *glr3.3 glr3.6* mutant. Bars represent SEM (n=24).

B) Fecundity is not altered on the *tpc1-2* mutant. Bars represent SEM (n=12).

C) Fecundity is not altered on the *35S:TCP1 5.6* line. Bars represent SEM (n=12).

D) Fecundity is significantly reduced on the *fou2* mutant, and can be rescued on the *fou2 aos* double mutant. Bars represent SEM (n=16).

Figure 11. Proposed model of Ca^{2+} release during *M. persicae* feeding.

Aphid image taken from Hogenhout and Bos (2011). (1) Aphids typically probe epidermal and mesophyll cell layers within 31 s of the start of feeding. (2) An aphid-induced $[Ca^{2+}]_{cyt}$ elevation can be detected around the feeding site within 95 s of settling that spreads to adjacent cells. (3) This $[Ca^{2+}]_{cyt}$ elevation is not detected systemically beyond the feeding site. (4) BAK1 and an unknown receptor (PRR) perceive aphid herbivore-associated molecular patterns (HAMPs) (Prince et al., 2014). (5) Perception of aphid HAMPs by BAK1 leads to activation of GLR3.3/GLR3.6, potentially through the release of glutamate (Chiu et al., 2002, Qi et al., 2006, Forde and Lea, 2007, Stephens et al., 2008). (6) GLR3.3/GLR3.6 mediate extracellular Ca^{2+} influx into the cell (Tapken and Hollmann, 2008, Vincill et al., 2012). (7) The increase in $[Ca^{2+}]_{cyt}$ results in activation of TPC1 (Hedrich and Neher, 1987, Ward and Schroeder, 1994). (8) TPC1, either directly or indirectly mediates release of intracellular Ca^{2+} from the vacuole (Peiter et al., 2005). (9) The increase in $[Ca^{2+}]_{cyt}$ may result in the activation of plant immunity against aphids, which can be enhanced by over-activation of TPC1. (10) During compatible interactions, such as that between Arabidopsis and *M.* persicae, the aphid supresses plant immunity using effectors (Bos et al., 2010, Mugford et al., 2016), which might also supresses $[Ca^{2+}]_{cyt}$ elevations.

Parsed Citations

AIDEMARK, M., ANDERSSON, C. J., RASMUSSON, A. G. & WIDELL, S. 2009. Regulation of callose synthase activity in situ in alamethicin-permeabilized Arabidopsis and tobacco suspension cells. Bmc Plant Biology, 9.Artn 27

Pubmed: Author and Title
CrossRef: Author and Title
Google Scholar: Author Only Title Only Author and Title

10.1186/1471-2229-9-27

ALLEN, G. J., CHU, S. P., SCHUMACHER, K., SHIMAZAKI, C. T., VAFEADOS, D., KEMPER, A., HAWKE, S. D., TALLMAN, G., TSIEN, R. Y., HARPER, J. F., CHORY, J. & SCHROEDER, J. I. 2000. Alteration of stimulus-specific guard cell calcium oscillations and stomatal closing in Arabidopsis det3 mutant. Science, 289, 2338-2342.DOI 10.1126/science.289.5488.2338

Pubmed: Author and Title
CrossRef: Author and Title
Google Scholar: Author Only Title Only Author and Title

ALLEN, G. J. & SANDERS, D. 1996. Control of ionic currents in guard cell vacuoles by cytosolic and luminal calcium. Plant Journal, 10, 1055-1069.DOI 10.1046/j.1365-313X.1996.10061055.x

Pubmed: Author and Title
CrossRef: Author and Title
Google Scholar: Author Only Title Only Author and Title

ATAMIAN, H. S., CHAUDHARY, R., DAL CIN, V., BAO, E., GIRKE, T. & KALOSHIAN, I. 2013. In Planta expression or delivery of potato aphid Macrosiphum euphorbiae effectors Me10 and Me23 enhances aphid fecundity. Molecular Plant-Microbe Interactions, 26, 67-74.10.1094/Mpmi-06-12-0144-Fi

Pubmed: Author and Title
CrossRef: Author and Title
Google Scholar: Author Only Title Only Author and Title

BLACKMAN, R. L. & EASTOP, V. F. 2000. Aphids on the world's crops: an identification and information guide, Chichester, UK, John Wiley & Sons, Ltd

BLACKMAN, R. L. & EASTOP, V. F. 2007. Taxonomic Issues. In: VAN EMDEN, H. F. & HARRINGTON, R. (eds.) Aphids as Crop Pests. Wallingford, UK: CABI.

Pubmed: Author and Title
CrossRef: Author and Title
Google Scholar: Author Only Title Only Author and Title

BLUME, B., NURNBERGER, T., NASS, N. & SCHEEL, D. 2000. Receptor-mediated increase in cytoplasmic free calcium required for activation of pathogen defense in parsley. Plant Cell, 12, 1425-1440.DOI 10.1105/tpc.12.8.1425

Pubmed: Author and Title
CrossRef: Author and Title
Google Scholar: Author Only Title Only Author and Title

BONAVENTURE, G., GFELLER, A., PROEBSTING, W. M., HORTENSTEINER, S., CHETELAT, A., MARTINOIA, E. & FARMER, E. E. 2007a. A gain-of-function allele of TPC1 activates oxylipin biogenesis after leaf wounding in Arabidopsis. Plant Journal, 49, 889-898.DOI 10.1111/j.1365-313X.2006.03002.x

Pubmed: Author and Title
CrossRef: Author and Title
Google Scholar: Author Only Title Only Author and Title

BONAVENTURE, G., GFELLER, A., RODRIGUEZ, V. M., ARMAND, F. & FARMER, E. E. 2007b. The fou2 gain-of-function allele and the wild-type allele of two pore channel 1 contribute to different extents or by different mechanisms to defense gene expression in Arabidopsis. Plant Cell Physiol, 48, 1775-89.10.1093/pcp/pcm151

Pubmed: Author and Title
CrossRef: Author and Title
Google Scholar: Author Only Title Only Author and Title

BOS, J. I., PRINCE, D., PITINO, M., MAFFEI, M. E., WIN, J. & HOGENHOUT, S. A. 2010. A functional genomics approach identifies candidate effectors from the aphid species Myzus persicae (green peach aphid). PLoS Genet, 6, e1001216.10.1371/journal.pgen.1001216

Pubmed: Author and Title
CrossRef: Author and Title
Google Scholar: Author Only Title Only Author and Title

BRICCHI, I., BERTEA, C. M., OCCHIPINTI, A., PAPONOV, I. A. & MAFFEI, M. E. 2012. Dynamics of membrane potential variation and gene expression induced by Spodoptera littoralis, Myzus persicae, and Pseudomonas syringae in Arabidopsis. PLoS One, 7, e46673.10.1371/journal.pone.0046673

Pubmed: Author and Title
CrossRef: Author and Title
Google Scholar: Author Only Title Only Author and Title

CAROLAN, J. C., FITZROY, C. I. J., ASHTON, P. D., DOUGLAS, A. E. & WILKINSON, T. L. 2009. The secreted salivary proteome of the pea aphid Acyrthosiphon pisum characterised by mass spectrometry. Proteomics, 9, 2457-2467.10.1002/pmic.200800692

Pubmed: Author and Title
CrossRef: Author and Title
Google Scholar: Author Only Title Only Author and Title

CHARPENTIER, M., SUN, J. H., MARTINS, T. V., RADHAKRISHNAN, G. V., FINDLAY, K., SOUMPOUROU, E., THOUIN, J., VERY, A. A., SANDERS, D., MORRIS, R. J. & OLDROYD, G. E. D. 2016. Nuclear-localized cyclic nucleotide-gated channels mediate symbiotic calcium oscillations. Science, 352, 1102-1105.10.1126/science.aae0109

Pubmed: Author and Title
CrossRef: Author and Title
Google Scholar: Author Only Title Only Author and Title

CHAUDHARY, R., ATAMIAN, H. S., SHEN, Z. X., BRIGG, S. P. & KALOSHIAN, I. 2014. GroEL from the endosymbiont Buchnera aphidicola betrays the aphid by triggering plant defense. Proceedings of the National Academy of Sciences of the United States of America, 111, 8919-8924.10.1073/pnas.1407687111

Pubmed: Author and Title
CrossRef: Author and Title
Google Scholar: Author Only Title Only Author and Title

CHEN, J. Q., RAHBE, Y., DELOBEL, B., SAUVION, N., GUILLAUD, J. & FEBVAY, G. 1997. Melon resistance to the aphid Aphis gossypii: behavioural analysis and chemical correlations with nitrogenous compounds. Entomologia Experimentalis Et Applicata, 85, 33-44.DOI 10.1046/j.1570-7458.1997.00232.x

Pubmed: Author and Title
CrossRef: Author and Title
Google Scholar: Author Only Title Only Author and Title

CHINCHILLA, D., BAUER, Z., REGENASS, M., BOLLER, T. & FELIX, G. 2006. The Arabidopsis receptor kinase FLS2 binds flg22 and determines the specificity of flagellin perception. Plant Cell, 18, 465-476.10.1105/tpc.105.036574

Pubmed: Author and Title
CrossRef: Author and Title
Google Scholar: Author Only Title Only Author and Title

CHINCHILLA, D., ZIPFEL, C., ROBATZEK, S., KEMMERLING, B., NURNBERGER, T., JONES, J. D. G., FELIX, G. & BOLLER, T. 2007. A flagellin-induced complex of the receptor FLS2 and BAK1 initiates plant defence. Nature, 448, 497-U12.10.1038/nature05999

Pubmed: Author and Title
CrossRef: Author and Title
Google Scholar: Author Only Title Only Author and Title

CHIU, J. C., BRENNER, E. D., DESALLE, R., NITABACH, M. N., HOLMES, T. C. & CORUZZI, G. M. 2002. Phylogenetic and expression analysis of the glutamate-receptor-like gene family in Arabidopsis thaliana. Molecular Biology and Evolution, 19, 1066-1082

Pubmed: Author and Title
CrossRef: Author and Title
Google Scholar: Author Only Title Only Author and Title

CHOI, W. G., HILLEARY, R., SWANSON, S. J., KIM, S. H. & GILROY, S. 2016. Rapid, long-distance electrical and calcium signaling in plants. Annual Review of Plant Biology, Vol 67, 67, 287-307.10.1146/annurev-arplant-043015-112130

Pubmed: Author and Title
CrossRef: Author and Title
Google Scholar: Author Only Title Only Author and Title

CHOI, W. G., TOYOTA, M., KIM, S. H., HILLEARY, R. & GILROY, S. 2014. Salt stress-induced Ca2+ waves are associated with rapid, long-distance root-to-shoot signaling in plants. Proc Natl Acad Sci U S A.10.1073/pnas.1319955111

Pubmed: Author and Title
CrossRef: Author and Title
Google Scholar: Author Only Title Only Author and Title

CLOUGH, S. J., FENGLER, K. A., YU, I. C., LIPPOK, B., SMITH, R. K. & BENT, A. F. 2000. The Arabidopsis dnd1 "defense, no death" gene encodes a mutated cyclic nucleotide-gated ion channel. Proceedings of the National Academy of Sciences of the United States of America, 97, 9323-9328.DOI 10.1073/pnas.150005697

Pubmed: Author and Title
CrossRef: Author and Title
Google Scholar: Author Only Title Only Author and Title

CONN, S. J., CONN, V., TYERMAN, S. D., KAISER, B. N., LEIGH, R. A. & GILLIHAM, M. 2011a. Magnesium transporters, MGT2/MRS2-1 and MGT3/MRS2-5, are important for magnesium partitioning within Arabidopsis thaliana mesophyll vacuoles. New Phytologist, 190, 583-594.10.1111/j.1469-8137.2010.03619.x

Pubmed: Author and Title
CrossRef: Author and Title
Google Scholar: Author Only Title Only Author and Title

CONN, S. J., GILLIHAM, M., ATHMAN, A., SCHREIBER, A. W., BAUMANN, U., MOLLER, I., CHENG, N. H., STANCOMBE, M. A., HIRSCHI, K. D., WEBB, A. A. R., BURTON, R., KAISER, B. N., TYERMAN, S. D. & LEIGH, R. A. 2011b. Cell-Specific vacuolar calcium storage mediated by CAX1 regulates apoplastic calcium concentration, gas exchange, and plant productivity in Arabidopsis. Plant Cell, 23, 240-257.10.1105/tpc.109.072769

Pubmed: Author and Title
CrossRef: Author and Title
Google Scholar: Author Only Title Only Author and Title

CONRATH, U. 2011. Molecular aspects of defence priming. Trends in Plant Science, 16, 524-531.10.1016/j.tplants.2011.06.004

Pubmed: Author and Title
CrossRef: Author and Title
Google Scholar: Author Only Title Only Author and Title

DIXON, A. 1998. Aphid Ecology: An Optimization Approach, London, Springer

DODD, A. N., KUDLA, J. & SANDERS, D. 2010. The language of calcium signaling. Annual Review of Plant Biology, Vol 61, 61, 593-620.DOI 10.1146/annurev-arplant-070109-104628
Pubmed: Author and Title
CrossRef: Author and Title
Google Scholar: Author Only Title Only Author and Title

DUBIELLA, U., SEYBOLD, H., DURIAN, G., KOMANDER, E., LASSIG, R., WITTE, C. P., SCHULZE, W. X. & ROMEIS, T. 2013. Calcium-dependent protein kinase/NADPH oxidase activation circuit is required for rapid defense signal propagation. Proceedings of the National Academy of Sciences of the United States of America, 110, 8744-8749.DOI 10.1073/pnas.1221294110
Pubmed: Author and Title
CrossRef: Author and Title
Google Scholar: Author Only Title Only Author and Title

EHRHARDT, D. W., WAIS, R. & LONG, S. R. 1996. Calcium spiking in plant root hairs responding to Rhizobium nodulation signals. Cell, 85, 673-681.Doi 10.1016/S0092-8674(00)81234-9
Pubmed: Author and Title
CrossRef: Author and Title
Google Scholar: Author Only Title Only Author and Title

ELLIS, C., KARAFYLLIDIS, L. & TURNER, J. G. 2002. Constitutive activation of jasmonate signaling in an Arabidopsis mutant correlates with enhanced resistance to Erysiphe cichoracearum, Pseudomonas syringae, and Myzus persicae. Molecular Plant-Microbe Interactions, 15, 1025-1030.10.1094/mpmi.2002.15.10.1025
Pubmed: Author and Title
CrossRef: Author and Title
Google Scholar: Author Only Title Only Author and Title

ELZINGA, D. A., DE VOS, M. & JANDER, G. 2014. Suppression of plant defenses by a Myzus persicae (green peach aphid) salivary effector protein. Molecular Plant-Microbe Interactions, 27, 747-756.10.1094/Mpmi-01-14-0018-R
Pubmed: Author and Title
CrossRef: Author and Title
Google Scholar: Author Only Title Only Author and Title

ESAU, K. 1977. Phloem. Anatomy of Seed Plants
Pubmed: Author and Title
CrossRef: Author and Title
Google Scholar: Author Only Title Only Author and Title

London: John Wiley and Sons.

EVANS, M. J., CHOI, W. G., GILROY, S. & MORRIS, R. J. 2016. A ROS-assisted calcium wave dependent on atrbohd and tpc1 propagates the systemic response to salt stress in Arabidopsis roots. Plant Physiol, 171, 1771-84.10.1104/pp.16.00215
Pubmed: Author and Title
CrossRef: Author and Title
Google Scholar: Author Only Title Only Author and Title

FORDE, B. G. & LEA, P. J. 2007. Glutamate in plants: metabolism, regulation, and signalling. Journal of Experimental Botany, 58, 2339-2358.10.1093/jxb/erm121
Pubmed: Author and Title
CrossRef: Author and Title
Google Scholar: Author Only Title Only Author and Title

FOYER, C. H., VERRALL, S. R. & HANCOCK, R. D. 2015. Systematic analysis of phloem-feeding insect-induced transcriptional reprogramming in Arabidopsis highlights common features and reveals distinct responses to specialist and generalist insects. Journal of Experimental Botany, 66, 495-512.10.1093/jxb/eru491
Pubmed: Author and Title
CrossRef: Author and Title
Google Scholar: Author Only Title Only Author and Title

FURCH, A. C. U., VAN BEL, A. J. E., FRICKER, M. D., FELLE, H. H., FUCHS, M. & HAFKE, J. B. 2009. Sieve element Ca2+ channels as relay stations between remote stimuli and sieve tube occlusion in Vicia faba. Plant Cell, 21, 2118-2132.10.1105/tpc.108.063107
Pubmed: Author and Title
CrossRef: Author and Title
Google Scholar: Author Only Title Only Author and Title

GALAN, J. E., LARA-TEJERO, M., MARLOVITS, T. C. & WAGNER, S. 2014. Bacterial type III secretion systems: specialized nanomachines for protein delivery into target cells. Annual Review of Microbiology, Vol 68, 68, 415-438.10.1146/annurev-micro-092412-155725
Pubmed: Author and Title
CrossRef: Author and Title
Google Scholar: Author Only Title Only Author and Title

GELLI, A., HIGGINS, V. J. & BLUMWALD, E. 1997. Activation of plant plasma membrane Ca2+-permeable channels by race-specific fungal elicitors. Plant Physiology, 113, 269-279
Pubmed: Author and Title
CrossRef: Author and Title
Google Scholar: Author Only Title Only Author and Title

GFELLER, A., BAERENFALLER, K., LOSCOS, J., CHETELAT, A., BAGINSKY, S. & FARMER, E. E. 2011. Jasmonate controls polypeptide patterning in undamaged tissue in wounded Arabidopsis leaves. Plant Physiol, 156, 1797-807.10.1104/pp.111.181008
Pubmed: Author and Title

CrossRef: Author and Title
Google Scholar: Author Only Title Only Author and Title

GILLIHAM, M., ATHMAN, A., TYERMAN, S. D. & CONN, S. J. 2011. Cell-specific compartmentation of mineral nutrients is an essential mechanism for optimal plant productivity-another role for TPC1? Plant Signal Behav, 6, 1656-61.10.4161/psb.6.11.17797
Pubmed: Author and Title
CrossRef: Author and Title
Google Scholar: Author Only Title Only Author and Title

GILROY, S., BIALASEK, M., SUZUKI, N., GORECKA, M., DEVIREDDY, A. R., KARPINSKI, S. & MITTLER, R. 2016. ROS, calcium, and electric signals: key mediators of rapid systemic signaling in plants. Plant Physiol, 171, 1606-15.10.1104/pp.16.00434
Pubmed: Author and Title
CrossRef: Author and Title
Google Scholar: Author Only Title Only Author and Title

GRADOGNA, A., SCHOLZ-STARKE, J., GUTLA, P. V. & CARPANETO, A. 2009. Fluorescence combined with excised patch: measuring calcium currents in plant cation channels. Plant J, 58, 175-82.10.1111/j.1365-313X.2008.03762.x
Pubmed: Author and Title
CrossRef: Author and Title
Google Scholar: Author Only Title Only Author and Title

GUO, J., ZENG, W., CHEN, Q., LEE, C., CHEN, L., YANG, Y., CANG, C., REN, D. & JIANG, Y. 2016. Structure of the voltage-gated two-pore channel TPC1 from Arabidopsis thaliana. Nature, 531, 196-201.10.1038/nature16446
Pubmed: Author and Title
CrossRef: Author and Title
Google Scholar: Author Only Title Only Author and Title

GUO, J., ZENG, W. & JIANG, Y. 2017. Tuning the ion selectivity of two-pore channels. Proceedings of the National Academy of Sciences.10.1073/pnas.1616191114
Pubmed: Author and Title
CrossRef: Author and Title
Google Scholar: Author Only Title Only Author and Title

HEDRICH, R. & NEHER, E. 1987. Cytoplasmic calcium regulates voltage-dependent ion channels in plant vacuoles. Nature, 329, 833-836.DOI 10.1038/329833a0
Pubmed: Author and Title
CrossRef: Author and Title
Google Scholar: Author Only Title Only Author and Title

HEESE, A., HANN, D. R., GIMENEZ-IBANEZ, S., JONES, A. M. E., HE, K., LI, J., SCHROEDER, J. I., PECK, S. C. & RATHJEN, J. P. 2007. The receptor-like kinase SERK3/BAK1 is a central regulator of innate immunity in plants. Proceedings of the National Academy of Sciences of the United States of America, 104, 12217-12222.10.1073/pnas.0705306104
Pubmed: Author and Title
CrossRef: Author and Title
Google Scholar: Author Only Title Only Author and Title

HOGENHOUT, S. A. & BOS, J. I. B. 2011. Effector proteins that modulate plant-insect interactions. Current Opinion in Plant Biology, 14, 422-428.DOI 10.1016/j.pbi.2011.05.003
Pubmed: Author and Title
CrossRef: Author and Title
Google Scholar: Author Only Title Only Author and Title

JAOUANNET, M., MORRIS, J. A., HEDLEY, P. E. & BOS, J. I. 2015. Characterization of arabidopsis transcriptional responses to different aphid species reveals genes that contribute to host susceptibility and non-host resistance. PLoS Pathog, 11, e1004918.10.1371/journal.ppat.1004918
Pubmed: Author and Title
CrossRef: Author and Title
Google Scholar: Author Only Title Only Author and Title

JEWORUTZKI, E., ROELFSEMA, M. R. G., ANSCHUTZ, U., KROL, E., ELZENGA, J. T. M., FELIX, G., BOLLER, T., HEDRICH, R. & BECKER, D. 2010. Early signaling through the Arabidopsis pattern recognition receptors FLS2 and EFR involves Ca2+-associated opening of plasma membrane anion channels. Plant Journal, 62, 367-378.10.1111/j.1365-313X.2010.04155.x
Pubmed: Author and Title
CrossRef: Author and Title
Google Scholar: Author Only Title Only Author and Title

JONES, J. D. G. & DANGL, J. L. 2006. The plant immune system. Nature, 444, 323-329.Doi 10.1038/Nature05286
Pubmed: Author and Title
CrossRef: Author and Title
Google Scholar: Author Only Title Only Author and Title

KAUSS, H., KOHLE, H. & JEBLICK, W. 1983. Proteolytic activation and stimulation by Ca2+ of glucan synthase from soybean cells. Febs Letters, 158, 84-88.Doi 10.1016/0014-5793(83)80681-4
Pubmed: Author and Title
CrossRef: Author and Title
Google Scholar: Author Only Title Only Author and Title

KEINATH, N. F., WAADT, R., BRUGMAN, R., SCHROEDER, J. I., GROSSMANN, G., SCHUMACHER, K. & KREBS, M. 2015. Live cell imaging with R-GECO1 sheds light on flg22- and chitin-induced transient [Ca2+]cyt patterns in Arabidopsis. Mol Plant, 8, 1188-200.10.1016/j.molp.2015.05.006

Pubmed: Author and Title
CrossRef: Author and Title
Google Scholar: Author Only Title Only Author and Title

KETTLES, G. J., DRUREY, C., SCHOONBEEK, H. J., MAULE, A. J. & HOGENHOUT, S. A. 2013. Resistance of Arabidopsis thaliana to the green peach aphid, Myzus persicae, involves camalexin and is regulated by microRNAs. New Phytol, 198, 1178-90.10.1111/nph.12218

Pubmed: Author and Title
CrossRef: Author and Title
Google Scholar: Author Only Title Only Author and Title

KETTLES, G. J. & KALOSHIAN, I. 2016. The Potato Aphid Salivary Effector Me47 Is a Glutathione-S-Transferase Involved in Modifying Plant Responses to Aphid Infestation. Frontiers in Plant Science, 7.ARTN 1142

Pubmed: Author and Title
CrossRef: Author and Title
Google Scholar: Author Only Title Only Author and Title

10.3389/fpls.2016.01142

Pubmed: Author and Title
CrossRef: Author and Title
Google Scholar: Author Only Title Only Author and Title

KIEGLE, E., MOORE, C. A., HASELOFF, J., TESTER, M. A. & KNIGHT, M. R. 2000. Cell-type-specific calcium responses to drought, salt and cold in the Arabidopsis root. Plant Journal, 23, 267-278.DOI 10.1046/j.1365-313x.2000.00786.x

Pubmed: Author and Title
CrossRef: Author and Title
Google Scholar: Author Only Title Only Author and Title

KIEP, V., VADASSERY, J., LATTKE, J., MAASS, J. P., BOLAND, W., PEITER, E. & MITHOFER, A. 2015. Systemic cytosolic Ca2+ elevation is activated upon wounding and herbivory in Arabidopsis. New Phytol, 207, 996-1004.10.1111/nph.13493

Pubmed: Author and Title
CrossRef: Author and Title
Google Scholar: Author Only Title Only Author and Title

KINTZER, A. F. & STROUD, R. M. 2016. Structure, inhibition and regulation of two-pore channel TPC1 from Arabidopsis thaliana. Nature, 531, 258-262.10.1038/nature17194

Pubmed: Author and Title
CrossRef: Author and Title
Google Scholar: Author Only Title Only Author and Title

KNIGHT, H. & KNIGHT, M. R. 2000. Imaging spatial and cellular characteristics of low temperature calcium signature after cold acclimation in Arabidopsis. Journal of Experimental Botany, 51, 1679-1686.DOI 10.1093/jexbot/51.351.1679

Pubmed: Author and Title
CrossRef: Author and Title
Google Scholar: Author Only Title Only Author and Title

KNIGHT, H., TREWAVAS, A. J. & KNIGHT, M. R. 1996. Cold calcium signaling in Arabidopsis involves two cellular pools and a change in calcium signature after acclimation. Plant Cell, 8, 489-503

Pubmed: Author and Title
CrossRef: Author and Title
Google Scholar: Author Only Title Only Author and Title

KNIGHT, M. R., CAMPBELL, A. K., SMITH, S. M. & TREWAVAS, A. J. 1991. Transgenic plant aequorin reports the effects of touch and cold-shock and elicitors on cytoplasmic calcium. Nature, 352, 524-526.DOI 10.1038/352524a0

Pubmed: Author and Title
CrossRef: Author and Title
Google Scholar: Author Only Title Only Author and Title

KNOBLAUCH, M., NOLL, G. A., MULLER, T., PRUFER, D., SCHNEIDER-HUTHER, I., SCHARNER, D., VAN BEL, A. J. E. & PETERS, W. S. 2003. ATP-independent contractile proteins from plants. Nature Materials, 2, 600-603.10.1038/nmat960

Pubmed: Author and Title
CrossRef: Author and Title
Google Scholar: Author Only Title Only Author and Title

KNOBLAUCH, M., PETERS, W. S., EHLERS, K. & VAN BEL, A. J. E. 2001. Reversible calcium-regulated stopcocks in legume sieve tubes. Plant Cell, 13, 1221-1230.DOI 10.1105/tpc.13.5.1221

Pubmed: Author and Title
CrossRef: Author and Title
Google Scholar: Author Only Title Only Author and Title

KOSUTA, S., HAZLEDINE, S., SUN, J., MIWA, H., MORRIS, R. J., DOWNIE, J. A. & OLDROYD, G. E. D. 2008. Differential and chaotic calcium signatures in the symbiosis signaling pathway of legumes. Proceedings of the National Academy of Sciences of the United States of America, 105, 9823-9828.10.1073/pnas.0803499105

Pubmed: Author and Title
CrossRef: Author and Title
Google Scholar: Author Only Title Only Author and Title

KUSNIERCZYK, A., TRAN, D. H., WINGE, P., JORSTAD, T. S., REESE, J. C., TROCZYNSKA, J. & BONES, A. M. 2011. Testing the importance of jasmonate signalling in induction of plant defences upon cabbage aphid (Brevicoryne brassicae) attack. BMC Genomics, 12, 423.10.1186/1471-2164-12-423

Pubmed: Author and Title
CrossRef: Author and Title
Google Scholar: Author Only Title Only Author and Title

KWAAITAAL, M., HUISMAN, R., MAINTZ, J., REINSTADLER, A. & PANSTRUGA, R. 2011. Ionotropic glutamate receptor (iGluR)-like channels mediate MAMP-induced calcium influx in Arabidopsis thaliana. Biochemical Journal, 440, 355-365.Doi 10.1042/Bj20111112

Pubmed: Author and Title
CrossRef: Author and Title
Google Scholar: Author Only Title Only Author and Title

LECOURIEUX, D., LAMOTTE, O., BOURQUE, S., WENDEHENNE, D., MAZARS, C., RANJEVA, R. & PUGIN, A. 2005. Proteinaceous and oligosaccharidic elicitors induce different calcium signatures in the nucleus of tobacco cells. Cell Calcium, 38, 527-538.10.1016/j.ceca.2005.06.036

Pubmed: Author and Title
CrossRef: Author and Title
Google Scholar: Author Only Title Only Author and Title

LECOURIEUX, D., MAZARS, C., PAULY, N., RANJEVA, R. & PUGIN, A. 2002. Analysis and effects of cytosolic free calcium increases in response to elicitors in Nicotiana plumbaginifolia cells. Plant Cell, 14, 2627-2641.10.1105/tpc.005579

Pubmed: Author and Title
CrossRef: Author and Title
Google Scholar: Author Only Title Only Author and Title

MA, Y., WALKER, R. K., ZHAO, Y. C. & BERKOWITZ, G. A. 2012. Linking ligand perception by PEPR pattern recognition receptors to cytosolic Ca2+ elevation and downstream immune signaling in plants. Proceedings of the National Academy of Sciences of the United States of America, 109, 19852-19857.10.1073/pnas.1205448109

Pubmed: Author and Title
CrossRef: Author and Title
Google Scholar: Author Only Title Only Author and Title

MAFFEI, M., BOSSI, S., SPITELLER, D., MITHOFER, A. & BOLAND, W. 2004. Effects of feeding Spodoptera littoralis on lima bean leaves. I. Membrane potentials, intracellular calcium variations, oral secretions, and regurgitate components. Plant Physiology, 134, 1752-1762.DOI 10.1104/pp.103.034165

Pubmed: Author and Title
CrossRef: Author and Title
Google Scholar: Author Only Title Only Author and Title

MANZOOR, H., KELLONIEMI, J., CHILTZ, A., WENDEHENNE, D., PUGIN, A., POINSSOT, B. & GARCIA-BRUGGER, A. 2013. Involvement of the glutamate receptor AtGLR3.3 in plant defense signaling and resistance to Hyaloperonospora arabidopsidis. Plant J, Accepted Article.10.1111/tpj.12311

Pubmed: Author and Title
CrossRef: Author and Title
Google Scholar: Author Only Title Only Author and Title

MARTIN, B., COLLAR, J. L., TJALLINGII, W. F. & FERERES, A. 1997. Intracellular ingestion and salivation by aphids may cause the acquisition and inoculation of non-persistently transmitted plant viruses. Journal of General Virology, 78, 2701-2705

Pubmed: Author and Title
CrossRef: Author and Title
Google Scholar: Author Only Title Only Author and Title

MATHERS, T. C., CHEN, Y., KAITHAKOTTIL, G., LEGEAI, F., MUGFORD, S. T., BAA-PUYOULET, P., BRETAUDEAU, A., CLAVIJO, B., COLELLA, S., COLLIN, O., DALMAY, T., DERRIEN, T., FENG, H., GABALDÓN, T., JORDAN, A., JULCA, I., KETTLES, G. J., KOWITWANICH, K., LAVENIER, D., LENZI, P., LOPEZ-GOMOLLON, S., LOSKA, D., MAPLESON, D., MAUMUS, F., MOXON, S., PRICE, D. R. G., SUGIO, A., VAN MUNSTER, M., UZEST, M., WAITE, D., JANDER, G., TAGU, D., WILSON, A. C. C., VAN OOSTERHOUT, C., SWARBRECK, D. & HOGENHOUT, S. A. 2017. Rapid transcriptional plasticity of duplicated gene clusters enables a clonally reproducing aphid to colonise diverse plant species. Genome Biology, in prep.10.1186/s13059-016-1145-3

Pubmed: Author and Title
CrossRef: Author and Title
Google Scholar: Author Only Title Only Author and Title

MCAINSH, M. R., WEBB, A. A. R., TAYLOR, J. E. & HETHERINGTON, A. M. 1995. Stimulus-induced oscillations in guard-cell cytosolic-free calcium. Plant Cell, 7, 1207-1219.DOI 10.1105/tpc.7.8.1207

Pubmed: Author and Title
CrossRef: Author and Title
Google Scholar: Author Only Title Only Author and Title

MEIJERING, E., DZYUBACHYK, O. & SMAL, I. 2012. Methods for cell and particle tracking. Methods in Enzymology, 504, 183-200

Pubmed: Author and Title
CrossRef: Author and Title
Google Scholar: Author Only Title Only Author and Title

MITHOFER, A. & BOLAND, W. 2008. Recognition of herbivory-associated molecular patterns. Plant Physiol, 146, 825-31.10.1104/pp.107.113118

Pubmed: Author and Title
CrossRef: Author and Title
Google Scholar: Author Only Title Only Author and Title

MIYA, A., ALBERT, P., SHINYA, T., DESAKI, Y., ICHIMURA, K., SHIRASU, K., NARUSAKA, Y., KAWAKAMI, N., KAKU, H. & SHIBUYA, N. 2007. CERK1, a LysM receptor kinase, is essential for chitin elicitor signaling in Arabidopsis. Proceedings of the National Academy of Sciences of the United States of America, 104, 19613-19618.10.1073/pnas.0705147104

Pubmed: Author and Title
CrossRef: Author and Title
Google Scholar: Author Only Title Only Author and Title

MORENO, A., GARZO, E., FERNANDEZ-MATA, G., KASSEM, M., ARANDA, M. A. & FERERES, A. 2011. Aphids secrete watery saliva into plant tissues from the onset of stylet penetration. Entomologia Experimentalis Et Applicata, 139, 145-153.10.1111/j.1570-7458.2011.01117.x

Pubmed: Author and Title
CrossRef: Author and Title
Google Scholar: Author Only Title Only Author and Title

MOUSAVI, S. A., CHAUVIN, A., PASCAUD, F., KELLENBERGER, S. & FARMER, E. E. 2013. GLUTAMATE RECEPTOR-LIKE genes mediate leaf-to-leaf wound signalling. Nature, 500, 422-6.10.1038/nature12478

Pubmed: Author and Title
CrossRef: Author and Title
Google Scholar: Author Only Title Only Author and Title

MUGFORD, S. T., BARCLAY, E., DRUREY, C., FINDLAY, K. C. & HOGENHOUT, S. A. 2016. An immuno-suppressive aphid saliva protein is delivered into the cytosol of plant mesophyll cells during feeding. Molecular Plant-Microbe Interactions 29, 854-861.10.1101/071811

Pubmed: Author and Title
CrossRef: Author and Title
Google Scholar: Author Only Title Only Author and Title

MURASHIGE, T. & SKOOG, F. 1962. A revised medium for rapid growth and bio assays with tobacco tissue cultures. Physiologia Plantarum, 15, 473-497.DOI 10.1111/j.1399-3054.1962.tb08052.x

Pubmed: Author and Title
CrossRef: Author and Title
Google Scholar: Author Only Title Only Author and Title

MUSSER, R. O., HUM-MUSSER, S. M., EICHENSEER, H., PEIFFER, M., ERVIN, G., MURPHY, J. B. & FELTON, G. W. 2002. Caterpillar saliva beats plant defences - a new weapon emerges in the evolutionary arms race between plants and herbivores. Nature, 416, 599-600.DOI 10.1038/416599a

Pubmed: Author and Title
CrossRef: Author and Title
Google Scholar: Author Only Title Only Author and Title

NAESSENS, E., DUBREUIL, G., GIORDANENGO, P., BARON, O. L., MINET-KEBDANI, N., KELLER, H. & COUSTAU, C. 2015. A secreted MIF cytokine enables aphid feeding and represses plant immune responses. Current Biology, 25, 1898-1903.10.1016/j.cub.2015.05.047

Pubmed: Author and Title
CrossRef: Author and Title
Google Scholar: Author Only Title Only Author and Title

NAM, K. J. & HARDIE, J. 2012. Host acceptance by aphids: Probing and larviposition behaviour of the bird cherry-oat aphid, Rhopalosiphum padi on host and non-host plants. Journal of Insect Physiology, 58, 660-668.10.1016/j.jinsphys.2012.01.017

Pubmed: Author and Title
CrossRef: Author and Title
Google Scholar: Author Only Title Only Author and Title

PARK, J. H., HALITSCHKE, R., KIM, H. B., BALDWIN, I. T., FELDMANN, K. A. & FEYEREISEN, R. 2002. A knock-out mutation in allene oxide synthase results in male sterility and defective wound signal transduction in Arabidopsis due to a block in jasmonic acid biosynthesis. Plant Journal, 31, 1-12.DOI 10.1046/j.1365-313X.2002.01328.x

Pubmed: Author and Title
CrossRef: Author and Title
Google Scholar: Author Only Title Only Author and Title

PEITER, E., MAATHUIS, F. J. M., MILLS, L. N., KNIGHT, H., PELLOUX, J., HETHERINGTON, A. M. & SANDERS, D. 2005. The vacuolar Ca2+-activated channel TPC1 regulates germination and stomatal movement. Nature, 434, 404-408.Doi 10.1038/Nature03381

Pubmed: Author and Title
CrossRef: Author and Title
Google Scholar: Author Only Title Only Author and Title

PITINO, M., COLEMAN, A. D., MAFFEI, M. E., RIDOUT, C. J. & HOGENHOUT, S. A. 2011. Silencing of aphid genes by dsRNA feeding from plants. Plos One, 6.ARTN e25709

Pubmed: Author and Title
CrossRef: Author and Title
Google Scholar: Author Only Title Only Author and Title

10.1371/journal.pone.0025709

Pubmed: Author and Title
CrossRef: Author and Title
Google Scholar: Author Only Title Only Author and Title

PITINO, M. & HOGENHOUT, S. A. 2013. Aphid protein effectors promote aphid colonization in a plant species-specific manner. Molecular Plant-Microbe Interactions, 26, 130-139.10.1094/Mpmi-07-12-0172-Fi

Pubmed: Author and Title
CrossRef: Author and Title
Google Scholar: Author Only Title Only Author and Title

PRINCE, D. C., DRUREY, C., ZIPFEL, C. & HOGENHOUT, S. A. 2014. The leucine-rich repeat receptor-like kinase BRASSINOSTEROID INSENSITIVE1-ASSOCIATED KINASE1 and the cytochrome P450 PHYTOALEXIN DEFICIENT3 contribute to innate immunity to aphids in Arabidopsis. Plant Physiol, 164, 2207-19.10.1104/pp.114.235598

Pubmed: Author and Title
CrossRef: Author and Title
Google Scholar: Author Only Title Only Author and Title

QI, Z., STEPHENS, N. R. & SPALDING, E. P. 2006. Calcium entry mediated by GLR3.3, an Arabidopsis glutamate receptor with a broad agonist profile. Plant Physiology, 142, 963-971.10.1104/pp.106.088989

Pubmed: Author and Title
CrossRef: Author and Title
Google Scholar: Author Only Title Only Author and Title

QI, Z., VERMA, R., GEHRING, C., YAMAGUCHI, Y., ZHAO, Y. C., RYAN, C. A. & BERKOWITZ, G. A. 2010. Ca2+ signaling by plant Arabidopsis thaliana Pep peptides depends on AtPepR1, a receptor with guanylyl cyclase activity, and cGMP-activated Ca2+ channels. Proceedings of the National Academy of Sciences of the United States of America, 107, 21193-21198.10.1073/pnas.1000191107

Pubmed: Author and Title
CrossRef: Author and Title
Google Scholar: Author Only Title Only Author and Title

RANF, S., WUNNENBERG, P., LEE, J., BECKER, D., DUNKEL, M., HEDRICH, R., SCHEEL, D. & DIETRICH, P. 2008. Loss of the vacuolar cation channel, AtTPC1, does not impair Ca2+ signals induced by abiotic and biotic stresses. Plant Journal, 53, 287-299.DOI 10.1111/j.1365-313X.2007.03342.x

Pubmed: Author and Title
CrossRef: Author and Title
Google Scholar: Author Only Title Only Author and Title

RAO, S. A. K., CAROLAN, J. C. & WILKINSON, T. L. 2013. Proteomic Profiling of cereal aphid saliva reveals both ubiquitous and adaptive secreted proteins. Plos One, 8.ARTN e57413

Pubmed: Author and Title
CrossRef: Author and Title
Google Scholar: Author Only Title Only Author and Title

10.1371/journal.pone.0057413

Pubmed: Author and Title
CrossRef: Author and Title
Google Scholar: Author Only Title Only Author and Title

REN, G. W., WANG, X. F., CHEN, D., WANG, X. W. & LIU, X. D. 2014. Effects of aphids Myzus persicae on the changes of Ca2+ and H2O2 flux and enzyme activities in tobacco. Journal of Plant Interactions, 9, 883-888.10.1080/17429145.2014.982221

Pubmed: Author and Title
CrossRef: Author and Title
Google Scholar: Author Only Title Only Author and Title

SALVADOR-RECATALA, V. 2016. New roles for the GLUTAMATE RECEPTOR-LIKE 3.3, 3.5, and 3.6 genes as on/off switches of wound-induced systemic electrical signals. Plant Signal Behav, 11, e1161879.10.1080/15592324.2016.1161879

Pubmed: Author and Title
CrossRef: Author and Title
Google Scholar: Author Only Title Only Author and Title

SALVADOR-RECATALA, V. & TJALLINGII, W. F. 2015. A New Application of the Electrical Penetration Graph (EPG) for Acquiring and Measuring Electrical Signals in Phloem Sieve Elements. Jove-Journal of Visualized Experiments.ARTN e52826

Pubmed: Author and Title
CrossRef: Author and Title
Google Scholar: Author Only Title Only Author and Title

10.3791/52826

SARRIA, E., CID, M., GARZO, E. & FERERES, A. 2009. Excel workbook for automatic parameter calculation of EPG data. Computers and Electronics in Agriculture, 67, 35-42.10.1016/j.compag.2009.02.006

Pubmed: Author and Title
CrossRef: Author and Title
Google Scholar: Author Only Title Only Author and Title

SAUGE, M. H., KERVELLA, J. & RAHBE, Y. 1998. Probing behaviour of the green peach aphid Myzus persicae on resistant Prunus genotypes. Entomologia Experimentalis Et Applicata, 89, 223-232.DOI 10.1046/j.1570-7458.1998.00403.x

Pubmed: Author and Title
CrossRef: Author and Title
Google Scholar: Author Only Title Only Author and Title

SCHOONHOVEN, L., VAN LOON, J. J. A. & DICKE, M. 2005. Insect-Plant Biology. 2nd edn ed. Oxford: Oxford Univ. Press;.

Pubmed: Author and Title
CrossRef: Author and Title
Google Scholar: Author Only Title Only Author and Title

SCHWESSINGER, B., ROUX, M., KADOTA, Y., NTOUKAKIS, V., SKLENAR, J., JONES, A. & ZIPFEL, C. 2011. Phosphorylation-dependent differential regulation of plant growth, cell death, and innate immunity by the regulatory receptor-like kinase BAK1. PLoS Genet, 7, e1002046.10.1371/journal.pgen.1002046

Pubmed: Author and Title

CrossRef: Author and Title
Google Scholar: Author Only Title Only Author and Title

SINGH, A. & PAOLILLO, D. J. 1990. Role of calcium in the callose response of self-pollinated brassica stigmas. American Journal of Botany, 77, 128-133.Doi 10.2307/2444801
Pubmed: Author and Title
CrossRef: Author and Title
Google Scholar: Author Only Title Only Author and Title

STADLER, R. & SAUER, N. 1996. The Arabidopsis thaliana AtSUC2 gene is specifically expressed in companion cells. Botanica Acta, 109, 299-306
Pubmed: Author and Title
CrossRef: Author and Title
Google Scholar: Author Only Title Only Author and Title

STASWICK, P. E., SU, W. & HOWELL, S. H. 1992. Methyl jasmonate inhibition of root growth and induction of a leaf protein are decreased in an Arabidopsis thaliana mutant. Proc Natl Acad Sci U S A, 89, 6837-40
Pubmed: Author and Title
CrossRef: Author and Title
Google Scholar: Author Only Title Only Author and Title

STEPHENS, N. R., QI, Z. & SPALDING, E. P. 2008. Glutamate receptor subtypes evidenced by differences in desensitization and dependence on the GLR3.3 and GLR3.4 genes. Plant Physiology, 146, 529-538.10.1104/pp.107.108134
Pubmed: Author and Title
CrossRef: Author and Title
Google Scholar: Author Only Title Only Author and Title

TAPKEN, D. & HOLLMANN, M. 2008. Arabidopsis thaliana glutamate receptor ion channel function demonstrated by ion pore transplantation. Journal of Molecular Biology, 383, 36-48.10.1016/j.jmb.2008.06.076
Pubmed: Author and Title
CrossRef: Author and Title
Google Scholar: Author Only Title Only Author and Title

THOR, K. & PEITER, E. 2014. Cytosolic calcium signals elicited by the pathogen-associated molecular pattern flg22 in stomatal guard cells are of an oscillatory nature. New Phytologist, 204, 873-881.10.1111/nph.13064
Pubmed: Author and Title
CrossRef: Author and Title
Google Scholar: Author Only Title Only Author and Title

TIAN, L., HIRES, S. A., MAO, T., HUBER, D., CHIAPPE, M. E., CHALASANI, S. H., PETREANU, L., AKERBOOM, J., MCKINNEY, S. A., SCHREITER, E. R., BARGMANN, C. I., JAYARAMAN, V., SVOBODA, K. & LOOGER, L. L. 2009. Imaging neural activity in worms, flies and mice with improved GCaMP calcium indicators. Nature Methods, 6, 875-U113.10.1038/nmeth.1398
Pubmed: Author and Title
CrossRef: Author and Title
Google Scholar: Author Only Title Only Author and Title

TJALLINGII, W. F. 1978. Mechanoreceptors of the aphid labium. Entomologia Experimentalis Et Applicata, 24, 731-&
Pubmed: Author and Title
CrossRef: Author and Title
Google Scholar: Author Only Title Only Author and Title

TJALLINGII, W. F. 1985. lectrical nature of recorded signals during stylet penetration by aphids. Entomologia Experimentalis Et Applicata, 38, 177-186
Pubmed: Author and Title
CrossRef: Author and Title
Google Scholar: Author Only Title Only Author and Title

TJALLINGII, W. F. & ESCH, T. H. 1993. Fine-structure of aphid stylet routes in plant-tissues in correlation with EPG signals. Physiological Entomology, 18, 317-328.DOI 10.1111/j.1365-3032.1993.tb00604.x
Pubmed: Author and Title
CrossRef: Author and Title
Google Scholar: Author Only Title Only Author and Title

TRAW, M. B., KNISKERN, J. M. & BERGELSON, J. 2007. SAR increases fitness of Arabidopsis thaliana in the presence of natural bacterial pathogens. Evolution, 61, 2444-2449.10.1111/j.1558-5646.2007.00211.x
Pubmed: Author and Title
CrossRef: Author and Title
Google Scholar: Author Only Title Only Author and Title

VATSA, P., CHILTZ, A., BOURQUE, S., WENDEHENNE, D., GARCIA-BRUGGER, A. & PUGIN, A. 2011. Involvement of putative glutamate receptors in plant defence signaling and NO production. Biochimie, 93, 2095-2101.DOI 10.1016/j.biochi.2011.04.006
Pubmed: Author and Title
CrossRef: Author and Title
Google Scholar: Author Only Title Only Author and Title

VERRILLO, F., OCCHIPINTI, A., KANCHISWAMY, C. N. & MAFFEI, M. E. 2014. Quantitative analysis of herbivore-induced cytosolic calcium by using a cameleon (YC 3.6) calcium sensor in Arabidopsis thaliana. Journal of Plant Physiology, 171, 136-139.10.1016/j.jplph.2013.09.020
Pubmed: Author and Title
CrossRef: Author and Title
Google Scholar: Author Only Title Only Author and Title

VINCILL, E. D., BIECK, A. M. & SPALDING, E. P. 2012. Ca2+ conduction by an amino acid-gated ion channel related to glutamate receptors. Plant Physiology, 159, 40-46.10.1104/pp.112.197509
Pubmed: Author and Title
CrossRef: Author and Title
Google Scholar: Author Only Title Only Author and Title

WANG, Y., KANG, Y., MA, C., MIAO, R., WU, C., LONG, Y., GE, T., WU, Z., HOU, X., ZHANG, J. & QI, Z. 2017. CNGC2 Is a Ca2+ Influx Channel That Prevents Accumulation of Apoplastic Ca2+ in the Leaf. Plant Physiol, 173, 1342-1354.10.1104/pp.16.01222
Pubmed: Author and Title
CrossRef: Author and Title
Google Scholar: Author Only Title Only Author and Title

WANG, W., DAI, H. E., ZHANG, Y., CHANDRASEKAR, R., LUO, L., HIROMASA, Y., SHENG, C. Z., PENG, G. X., CHEN, S. L., TOMICH, J. M., REESE, J., EDWARDS, O., KANG, L., REECK, G. & CUI, F. 2015. Armet is an effector protein mediating aphid-plant interactions. Faseb Journal, 29, 2032-2045.10.1096/fj.14-266023
Pubmed: Author and Title
CrossRef: Author and Title
Google Scholar: Author Only Title Only Author and Title

WARD, J. M. & SCHROEDER, J. I. 1994. Calcium-activated K+ channels and calcium-induced calcium-release by slow vacuolar ion channels in guard-cell vacuoles implicated in the control of stomatal closure. Plant Cell, 6, 669-683
Pubmed: Author and Title
CrossRef: Author and Title
Google Scholar: Author Only Title Only Author and Title

WEILAND, M., MANCUSO, S. & BALUSKA, F. 2016. Signalling via glutamate and GLRs in Arabidopsis thaliana. Functional Plant Biology, 43, 1-25.10.1071/fp15109
Pubmed: Author and Title
CrossRef: Author and Title
Google Scholar: Author Only Title Only Author and Title

WILL, T., TJALLINGII, W. F., THONNESSEN, A. & VAN BEL, A. J. E. 2007. Molecular sabotage of plant defense by aphid saliva. Proceedings of the National Academy of Sciences of the United States of America, 104, 10536-10541.10.1073/pnas.0703535104
Pubmed: Author and Title
CrossRef: Author and Title
Google Scholar: Author Only Title Only Author and Title

WILL, T. & VAN BEL, A. J. E. 2006. Physical and chemical interactions between aphids and plants. Journal of Experimental Botany, 57, 729-737.Doi 10.1093/Jxb/Erj089
Pubmed: Author and Title
CrossRef: Author and Title
Google Scholar: Author Only Title Only Author and Title

XIONG, T. C., RONZIER, E., SANCHEZ, F., CORRATGE-FAILLIE, C., MAZARS, C. & THIBAUD, J. B. 2014. Imaging long distance propagating calcium signals in intact plant leaves with the BRET-based GFP-aequorin reporter. Front Plant Sci, 5, 43.10.3389/fpls.2014.00043
Pubmed: Author and Title
CrossRef: Author and Title
Google Scholar: Author Only Title Only Author and Title

YAMAGUCHI, Y., PEARCE, G. & RYAN, C. A. 2006. The cell surface leucine-rich repeat receptor for AtPep1, an endoaenous peptide elicitor in Arabidopsis, is functional in transgenic tobacco cells. Proceedings of the National Academy of Sciences of the United States of America, 103, 10104-10109.10.1073/pnas.0603729103
Pubmed: Author and Title
CrossRef: Author and Title
Google Scholar: Author Only Title Only Author and Title

YANG, D. H., HETTENHAUSEN, C., BALDWIN, I. T. & WU, J. Q. 2012. Silencing Nicotiana attenuata calcium-dependent protein kinases, CDPK4 and CDPK5, strongly up-regulates wound- and herbivory-induced jasmonic acid accumulations. Plant Physiology, 159, 1591-1607.10.1104/pp.112.199018
Pubmed: Author and Title
CrossRef: Author and Title
Google Scholar: Author Only Title Only Author and Title

YU, I. C., PARKER, J. & BENT, A. F. 1998. Gene-for-gene disease resistance without the hypersensitive response in Arabidopsis dnd1 mutant. Proceedings of the National Academy of Sciences of the United States of America, 95, 7819-7824.DOI 10.1073/pnas.95.13.7819
Pubmed: Author and Title
CrossRef: Author and Title
Google Scholar: Author Only Title Only Author and Title

ZHANG, X., XUE, M. & ZHAO, H. P. 2015. Species-specific effects on salicylic acid content and subsequent Myzus persicae (Sulzer) performance by three phloem-sucking insects infesting Nicotiana tabacum L. Arthropod-Plant Interactions, 9, 383-391.10.1007/s11829-015-9385-9
Pubmed: Author and Title
CrossRef: Author and Title
Google Scholar: Author Only Title Only Author and Title

ZHU, X., CAPLAN, J., MAMILLAPALLI, P., CZYMMEK, K., DINESH-KUMAR, S.P. 2010 Function of endoplasmic reticulum calcium

ATPase in innate immunity-mediated programmed cell death. EMBO J, 29(5), 1007-1018.
Pubmed: Author and Title
CrossRef: Author and Title
Google Scholar: Author Only Title Only Author and Title

ZIMMERMANN, S., NURNBERGER, T., FRACHISSE, J. M., WIRTZ, W., GUERN, J., HEDRICH, R. & SCHEEL, D. 1997. Receptor-mediated activation of a plant Ca2+-permeable ion channel involved in pathogen defense. Proceedings of the National Academy of Sciences of the United States of America, 94, 2751-2755.DOI 10.1073/pnas.94.6.2751
Pubmed: Author and Title
CrossRef: Author and Title
Google Scholar: Author Only Title Only Author and Title

ZIPFEL, C. 2009. Early molecular events in PAMP-triggered immunity. Current Opinion in Plant Biology, 12, 414-420.10.1016/j.pbi.2009.06.003
Pubmed: Author and Title
CrossRef: Author and Title
Google Scholar: Author Only Title Only Author and Title

ZIPFEL, C., KUNZE, G., CHINCHILLA, D., CANIARD, A., JONES, J. D. G., BOLLER, T. & FELIX, G. 2006. Perception of the bacterial PAMP EF-Tu by the receptor EFR restricts Agrobacterium-mediated transformation. Cell, 125, 749-760.10.1016/j.cell.2006.03.037
Pubmed: Author and Title
CrossRef: Author and Title
Google Scholar: Author Only Title Only Author and Title